Synthesis and Processing of Polymers for Biomedical Applications

by

Xiaoshu Dai

A Dissertation

Submitted to the Faculty of the

WORCESTER POLYTECHNIC INSTITUTE

In partial fulfillment of the requirements for the

Degree of Doctor of Philosophy

In

Material Science and Engineering

May 3rd 2010

APPROVED:

_____

Satya Shivkumar, Ph.D. Advisor
Professor of Mechanical Engineering
Worcester Polytechnic Institute

Richard D. Sisson, Jr., Ph.D.
George F. Fuller Professor of Mechanical Engineering
Director of Manufacturing and Materials Engineering
Dean of Graduate Studies
Worcester Polytechnic Institute

Thomas H. Jozefiak, Ph.D.
Genzyme Corporation

Art J. Coury, Ph.D.
Genzyme Corporation

TABLE OF CONTENTS

TABLE OF CONTENTS ..... **II**

ACKNOWLEDGEMENTS ..... **III**

ABSTRACT ..... **I**

CHAPTER 1: INTRODUCTION **3**

1.1 THESIS ORGANIZATION 3
1.2 INTRODUCTION 3
1.2.1 *IN SITU* FORMING HYDROGELS 3
1.2.2 ELECTROSPINNING 4
1.3 RESEARCH OBJECTIVES 5
1.4 METHODOLOGY 6

CHAPTER 2: BACKGROUND **10**

2.1. *IN SITU* FORMING HYDROGELS 10
2.2. EFFECTS OF MOLECULAR WEIGHT DISTRIBUTION (MWD) ON THE ELECTROSPINNING MORPHOLOGIES OF POLYMER SOLUTIONS 13
2.3. EFFECTS OF ADDITIVE ON ELECTROSPINNING OF POLYMER SOLUTIONS 17

CHAPTER 3: PUBLICATIONS **24**

FREE RADICAL POLYMERIZATION OF PEG-DIACRYLATE MACROMERS: IMPACT OF MACROMER HYDROPHOBICITY AND INITIATOR CHEMISTRY ON POLYMERIZATION EFFICIENCY 24
EFFECTS OF MOLECULAR WEIGHT DISTRIBUTION ON THE FORMATION OF FIBERS OF ELECTROSPUN POLYSTYRENE 53
MOLECULAR INTERACTIONS BETWEEN POLYVINYLPYRROLIDONE AND SURFACTANT: THE EFFECTS OF COIL DIMENSIONS ON ELECTROSPUN MORPHOLOGIES 66

CHAPTER 4 CONCLUSIONS **80**

ACKNOWLEDGEMENTS

I dedicate this thesis to my family: especially my parents, Lang Dai and Shangqing Wang for their love, support, and confidence in me through these years. They have my unconditional gratitude for their influence of my pursuit of graduate education and for being my inspiration and motivation of my life. I love them very much and can never thank them enough for all the opportunities they have given me.

My sincere appreciation goes to my advisor, Professor. Satya Shivkumar, for taking me as his graduate student, introducing and guiding me through the world of electrospinning. I would like to thank Professor Richard D. Sisson for being a great mentor during my graduate study. I would also like to thank Dr. Arthur J. Coury and Dr. Thomas H. Jozefiak for giving me an opportunity and experience of working in the industry. They are the true chemists: enthusiastic, creative, and inspirational. It was such a great honor to have these great scientists as my committee members. Their wide knowledge has provided a great basis for the present thesis. Their guidance and encouragement accompanied me during every step through the thesis work.

And last, but not least, my boyfriend, Anton Gurov, for all his love and support.

ABSTRACT

In situ polymerizing hydrogel systems play an important role in many tissue engineering applications. They have proven to be useful in biomedical applications that require conversion of liquid macromer solution to tissue compliant hydrogel under physiological conditions. A series of poly(ethylene glycol)-co-poly(lactate) diacrylate macromers were synthesized with variable PEG molecular weight and lactate content. The macromer compositions were confirmed by NMR spectroscopy and ion chromatography. These macromers were polymerized to form hydrogels by free radical polymerization using either redox or photochemical initiators. The current study focused on the optimization of polymerization conditions. Compressive modulus and residual acrylate analysis were used to evaluate polymerization efficiency. To characterize the network structure, the swelling ratio values were converted to the average molecular weight between crosslinks ($\overline{M_c}$) and mesh sizes (ξ) using Flory-Rehner theory. Current study suggested hydrophobic modification is desired to achieve high polymerization efficiency.

Electrospinning is a developing technique to produce ultra fine fibrous structures from polymer solutions. Current research efforts have focused on understanding the effects of principal parameters such as molecular weight distribution (MWD) and polymer surfactant interactions on the morphology of the electrospun patterns. Fundamental understanding of the dilute solution rheology of the polydisperse polymer/solvent and polymer/solvent/surfactant systems was first established. Using viscometry, the on-set of entanglement concentrations could be obtained for various systems. Electrospinning was then carried out to evaluate the effects of polymer molecular weight, molecular weight distribution (MWD) and the polymer-surfactant interaction on the fiber formation and morphological features. The importance of increased

chain entanglements due to high molecular weight component within the polydisperse system and the expansion of the coil dimension by binding the surfactant micelles have been recognized. The critical concentrations for incipient as well as stable fiber formation were determined.

CHAPTER 1: INTRODUCTION

1.1 Thesis Organization

This thesis is presented as a collection of various publications originating from this study. It is divided into four chapters. This introductory chapter serves to familiarize the reader with the motivations and goals that have driven this project. The second chapter is a literature review of relevant research which has facilitated the understanding of the basic principles upon which this project is based. The third chapter is a compilation of journal articles that have either been published or submitted to peer-reviewed journals. Finally, overall conclusions are presented in chapter four. In addition, a basic summary of the various methodologies used in the experiments are also presented. The specific details pertaining to the experiments are provided in the corresponding publications.

1.2 Introduction

1.2.1 *In situ* Forming Hydrogels

Hydrogels are three-dimensional, hydrophilic, polymeric, networks containing large amounts of water or biological fluids [1]. In the past decade, research interest has shifted from preformed hydrogel implants to injectable formulations that form a gel *in situ* under physiological conditions using minimally invasive techniques. *In situ* forming hydrogel compositions have been developed for diverse applications such as hemostats, tissue sealants, adhesion barriers, cell encapsulation, drug delivery and tissue engineering [2]. Several advantages include the possibilities to precisely control spatial application of the gel as well as the rate of gel formation. Cells and various therapeutic agents may be easily incorporated into

liquid hydrogel formulations. Most often *in situ* hydrogels are formed by the chemical crosslinking of water soluble polymers known as "macromers" to form swollen hydrophilic networks [2]. These water soluble macromers contain functionalities that enable polymerization by either step growth or chain growth mechanisms. Optionally, macromers can also contain chemical groups capable of degrading *in vivo* [3-5], thus customizing the residence time of the hydrogel to meet the needs of the intended application. Both natural and synthetic polymers can be used for the production of hydrogels. Poly(ethylene glycol) (PEG) is a synthetic polymer that has been used extensively in biomedical hydrogel systems due to its excellent biocompatibility. Many PEG derivatives capable of polymerization by free radical polymerization methods have been reported [6-8].

Initiation of the hydrogel forming polymerization reaction was demonstrated using either photochemical or redox methods. Despite the large number of studies employing hydrogels from PEG acrylate and methacrylate macromers by both photo chemistry and redox chemistry [8-10], few studies [11] have addressed the comparative polymerization efficiency for various initiators or the effect of macromer structural features that influence polymerization efficiency.

1.2.2 Electrospinning

Electrospinning is one of the major ways to engineer sub-micron non-woven fibrous structures [12]. The work of Taylor and others on electrically driven jets has laid the ground work for electrospinning [13]. The non-woven structures produced by electrospinning technique have unique features including interconnected pores and very high surface-to-volume ratio. These advantages enable these fibrous scaffolds to have many applications such as products for sensor technology [14], tissue scaffolds [15], drug delivery systems [16], filtration and protective clothing [17].

The stability of these non-woven structures depends on the polymer composition, solution properties and processing procedures. In the past few years, researchers have focused on developing and engineering the electrospinnabilities of new materials as well as the effects of process variables on the properties of the electrospun structures. Several studies on the relationship between viscosity, polymer concentration, and fiber formation showed a good correlation between solution regimes and the occurrence of beads, beaded and uniform fibers in electrospinning of polymer solutions [18]. However, these results only occur with polymers of narrow molecular weight distribution. It is necessary to study the dependence of the electrospun fibrous structures on polymer molecular weight distribution.

The interactions between surfactant and suitable polymers have attracted attention in the production of nanofibers by electrospinning [16]. A number of nonionic polymers have been electrospun with ionic surfactants as a co-spinning agent to form uniform fibrous structures [19-21]. The complexation between polymer and surfactant is best known to lead to a low surface tension and high solution conductivity which favor the stability of the solution jet and the formation of uniform fibrous structures [22-24]. Researchers have been focusing on the effects of surfactant on polymer electrospinnability with surfactant concentration around or well above the surfactant critical micelle concentration (CMC). It's important to establish systematic understanding of the effects of surfactant on solution rheology and electrospun polymer fibrous structures.

1.3 Research Objectives

The objectives of this work were:

- to examine the efficiency of polymerization for water-soluble and biodegradable macromers using free radical initiation chemistry

- to optimize the polymerization conditions
- to compare the physical properties and network structures of the resulting hydrogels.
- to study the effects of polymer molecular weight distribution (MWD) on electrospun fibers
- to determine the critical concentrations for incipient (c_i) as well as stable (c_e) fiber formation of electrospun polydisperse polymer solutions
- to study the effects of polymer surfactant interactions on polymer coil dimensions and electrospinning morphologies
- to determine the minimum effective surfactant concentration (c_m) for complete fiber formation

1.4 Methodology

Macromer synthesis and characterization: All modified poly(ethylene glycol) (PEG) based macromers were synthesized using a one-pot solution polymerization procedure. The purpose of this synthesis is to modify PEG diacrylate with 0 or an average of 6 lactate groups per chain. Macromer molecular weights (M_n and M_w) and polydispersity index (PDI) were determined using size exclusion chromatography (SEC). Macromer composition was verified using proton nuclear magnetic resonance (^{1}H NMR) spectroscopy and ion chromatography (IC). The critical micelle concentration (CMC) values for macromer solutions were determined using Static Light Scattering (SLS).

Hydrogel synthesis and characterization: Macromers were formulated by dissolution in deionized (DI) water at ambient temperature (21 ^{o}C) with concentrated redox and photo initiator solutions. Uniaxial compression experiments were performed on the cylindrical gel samples by

dynamic mechanical analysis (DMA) at 37 ^{o}C with a compression clamp. Three samples were tested for each polymerization condition. Averages and standard deviations were reported.

Swelling studies were performed to determine how much water a polymerized hydrogel would take up in a 24 hour period. Macromer polymerization was quantified by the determination of unreacted acrylic acid liberated from exhaustive hydrolysis of the hydrogels by ion chromatography (IC). The number average molecular weight between crosslinks ($\overline{M_c}$) and the mesh size (ξ) were also calculated.

Preparation of polydisperse polystyrene (published in the *Proceedings of the ANTEC^{TM} 2007*): Six nearly monodisperse polystyrene samples with M_w ranging from 19,300 - 1,877,000 g/mol were utilized to prepare a wide molecular weight distribution (MWD) sample with the desired polydispersities of 1.7, 2.5 and 3.3 while the number average molecular weights (M_n) were kept constant.

Viscosity measurements (published in the *Proceedings of the ANTEC^{TM} 2007):* The viscosity of the solutions at ambient temperature (21°C) was measured using a digital cone-plate rheometer (Brookfield Model DV III) equipped with a cone-spindle. The viscosity of the mixture was then measured at desired shear rates varied between 0.1s^{-1} and 250s^{-1}. The zero-shear viscosity (η_o) was calculated based on power law equation: $\eta=\eta_o \dot{\gamma}^{n-1}$, in which $\dot{\gamma}$ is the strain rate and n is the flow index.

Electrospinning (Submitted to the *Journal of Applied Polymer Science*)*:* The solution mixture was loaded in a 1mL syringe equipped with an 18 gauge needle. The syringe was mounted horizontally on a syringe pump (EW-74900-00, Cole-Parmer). A grounded aluminum foil collector (10 cm × 10 cm) was positioned 10 cm from the tip of the needle. The syringe

pump was calibrated to achieve a flow rate of 0.1 mL/h for all experiments. A desired potential voltage was applied to the needle immediately after a pendant drop formed at the tip. The electrospun samples were sputter coated with gold-palladium and examined in a JEOL JSM-7000F (Tokyo, Japan) scanning electron microscope (SEM).

Reference

1. N.A. Peppas, "Hydrogels and Drug Delivery," *Curr. Opinion Coll. Interfac. Sci.*, 2(1997)531-7.
2. S.R. Van Tomme, G. Storm, and W.E. Hennink, "*In Situ* Gelling Hydrogels for Pharmaceutical and Biomedical Applications," *Int. J. Pharm.*, 355(2008)1-18.
3. A.S. Sawhney, C.P. Pathak, and J.A. Hubbell, "Bioerodible Hydrogels based on Photopolymerized Poly(ethylene glycol)-co-Poly(α-hydroxy acid) Diacrylate macromers," *Macromolecules*, 26(1993)581-7.
4. J. Li, and W.J. Kao, "Synthesis of Polyethylene Glycol (PEG) Derivatives and PEGylated−Peptide Biopolymer Conjugates," *Biomacromolecules*, 4(2003)1055-67.
5. P.J. Martens, S.J. Bryant, and K.S. Anseth, "Tailoring the Degradation of Hydrogels Formed from Multivinyl Poly(ethylene glycol) and Poly(vinyl alcohol) Macromers for Cartilage Tissue Engineering," *Biomacromolecules*, 4(2003)283-92.
6. S. He, M.J. Yaszemski, A.W. Yasko, P.S. Engel, and A.G. Mikos, "Injectable Biodegradable Polymer Composites based on Poly(propylene fumarate) Crosslinked with Poly(ethylene glycol)-dimethacrylate," *Biomaterials*, 21(2000)2389-94.
7. F.M. Andreopoulos, E.J. Beckman, and A.J. Russell, "Light-induced Tailoring of PEG-Hydrogel Properties," *Biomaterials*, 19(1998)1343-52.
8. J.B. Leach, and C.E. Schmidt, "Characterization of Protein Release from Photocrosslinkable Hyaluronic Acid-Polyethylene glycol Hydrogel Tissue Engineering Scaffolds," *Biomaterials*, 26(2005)125-35.
9. W.E. Hennink, O. Franssen, W.N.E. van Dijk-Wolthuis, and H. Talsma, "Dextran Hydrogels for the Controlled Release of Proteins," *J. Controlled Release*, 48(1997)107-14.
10. D. Mawad, P.J. Martens, R.A. Odell, and L.A. Poole-Warren, "The Effect of Redox Polymerisation on Degradation and Cell Responses to Poly (vinyl alcohol) Hydrogels," *Biomaterials*, 28(2007)947-55.
11. D. Mawad, R. Odell, and L.A. Poole-Warren, "Network Structure and Macromolecular Drug Release from Poly(vinyl alcohol) Hydrogels Fabricated via Two Crosslinking Strategies," *Int. J. Pharm.*, 366(2009)31–7.
12. T. Liu, C. Burger, and B. Chu, "Nanofabrication in Polymer Matrices," *Progr. Polym. Sci.*, 28(2003) 5-26.
13. G.I. Taylor, "Disintegration of Water Drops in an Electric Field," *Proc. R. Soc. Lond. Ser. A,* 1382(1964) 383-97.
14. H. Fong, W. Liu, C.-S. Wang, and R.A. Vaia, "Generation of Electrospun Fibers of Nylon 6 and Nylon 6-Montmorillonite Nanocomposite," *Polymer*, 43(2001)775-80.

15. E.D. Boland, J.A. Matthews, K.J. Pawlowski, D.G. Simpson, G.E. Wnek, and G.L. Bowlin, "Electrospinning Collagen and Elastin: Preliminary Vascular Tissue Engineering ," *Front. Bioscience*, 9(2004)1422-32.
16. J. Zeng, X. Xu, X. Chen, Q. Liang, X. Bian, L. Yang, and X. Jing, "Biodegradable Electrospun Fibers for Drug Delivery," *J. Controlled Release*, 92(2003)227-31.
17. P. Gibson, H. Schreuder-Gibson, and C. Pentheny, "Electrospinning Technology: Direct Application of Tailorable Ultrathin Membranes," *J. Ind. Text.*, 28(1998)63-72.
18. P. Gupta, C. Elkins, T.E. Long, and G.L. Wilkes, "Electrospinning of Linear Homopolymers of Poly(methyl methacrylate): Exploring Relationships between Fiber Formation, Viscosity, Molecular Weight and Concentration in a Good Solvent," *Polymer*, 46 (2005) 4799-810.
19. N. Bhattarai, D. Edmondson, O. Veiseh, F.A. Matsen, and M. Zhang, "Electrospun Chitosan-based Nanofibers and Their Cellular Compatibility," *Biomaterials*, 26(2005)6176-84.
20. S.-Q. Wang, J.-H. He, and L. Xu, "Non-ionic Surfactants for Enhancing Electrospinability and for the Preparation of Electrospun Nanofibers," *Polym. Int.*, 57(2008)1079-82.
21. R. Nagarajan, C. Drew, and C.M. Mello, "Polymer−Micelle Complex as an Aid to Electrospinning Nanofibers from Aqueous Solutions," *J. Phys. Chem. C*, 111(2007)16105-8.
22. L. Yao, T.W. Haas, A. Guiseppi-Elie, G.L. Bowlin, D.G. Simpson, and G.E. Wnek, "Electrospinning and Stabilization of Fully Hydrolyzed Poly(Vinyl Alcohol) Fibers," *Chem. Mater.*, 15(2003)1860-4.
23. M. Pérez-Rodríguez, L.M. Varela, M. García, V. Mosquera, and F.J. Sarmiento, "Conductivity and Relative Permittivity of Sodium n-Dodecyl Sulfate and n-Dodecyl Trimethylammonium Bromide," *J. Chem. Eng. Data*, 44(1999)944-7.
24. C. Kriegel, K.M. Kit, D.J. McClements, and J. Weiss, "Electrospinning of Chitosan–Poly(ethylene oxide) Blend Nanofibers in the Presence of Micellar Surfactant Solutions," *Polymer*, 50(2009)189-200.

CHAPTER 2: BACKGROUND

2.1. *In Situ* Forming Hydrogels

Hydrogels are three-dimensional, hydrophilic, polymeric networks containing large amounts of imbibed water or biological fluids [1]. Since the introduction of hydrogels as soft contact lenses in the 1960s [1], their uses have increased tremendously and nowadays they are favored in a broad range of pharmaceutical and biomedical applications. In the past decade, research interest has shifted from preformed hydrogel implants to injectable formulations. These formulations can be introduced into the body prior to solidifying or gelling within the desired tissue, organ or body cavity. Many *in situ* forming hydrogel compositions have been developed in recent years for diverse applications such as hemostats, tissue sealants, adhesion barriers, cell encapsulation, drug delivery and tissue engineering [1-4]. *In situ* forming hydrogel systems are particularly advantageous for therapeutic modalities requiring injectable or minimally invasive application procedures. In many cases it is possible to precisely control spatial application of the gel as well as the rate of gel formation. Cells and various therapeutic agents may be easily incorporated into liquid hydrogel formulations. Often, *in situ* hydrogels are formed by chemical crosslinking of water soluble polymers known as "macromers" to form swollen hydrophilic networks [5]. These water soluble macromers contain functionalities that enable polymerization by either condensation or free radical mechanisms [6]. Optionally, macromers can also contain chemical groups capable of degrading *in vivo*, thus customizing the residence time of the hydrogel to meet the needs of the intended application.

Poly(ethylene glycol) (PEG) is a synthetic polymer that has been used extensively in biomedical hydrogel systems due to its excellent biocompatibility. Many PEG derivatives capable of polymerization by free radical polymerization methods have been reported, including:

meth/acrylates [7-10], fumarate [11], cinnamylidene acetate [12] and nitrocinnamate [13]. In many of these cases, the polymerizable PEG macromers also include functionality allowing for degradation *in vivo* such as lactate [14], glycolate [14], glutarate [15], or succinate [16]. Sperinde *et al*. [17] demonstrated the enzyme catalyzed synthesis of PEG-based hydrogel. Tetrahydroxy PEG was functionalized with glutaminyl groups. Hydrogel networks were formed by the addition of trans-glutaminase to aqueous solutions of functionalized PEG and poly(lysine-co-phenylalanine). It was reported that the properties of the gel could be tailored by the ratio of functionalized PEG and the lysine copolymer. In a more recent publication, the poly(lysine-co-phenylalanine) was replaced by lysine end-functionalized PEG. Hydrogels were obtained under similar physiological conditions [18].

Pioneering work in this area was performed by Hubbell and colleagues who synthesized macromers having a PEG central block, extended with oligomers of α-hydroxy acids and terminated with acrylate groups. Hydrogel was formed by radical polymerization of the acrylate groups on the macromers. These hydrogels were indeed biodegradable with PEG, lactic acid (or other α-hydroxy acids, depending on the macromer) and oligo(acrylic acid) as degradation end-products. The degradation time varied from 1 day to 4 months and could be tailored by the choice of macromer, especially by the choice of degradable link [14]. Metters *et al*. showed that the degradation could be accelerated by copolymerization of PEG-PLA macromers with acrylic acid [19].

Initiation of the hydrogel forming polymerization reaction was demonstrated using either photochemical or redox methods. Subsequent studies by Hubbell and other laboratories largely employed photochemical initiation. Radicals were generated after exposure to UV light of macromer aqueous solution to which a suitable photoinitiator was added. The convenience of

single-part formulation and the delicate control of the polymerization using light as an external stimulus lead to the popularity of photopolymerization application.

Balancing the many advantages of *in situ* hydrogel formation by photochemical initiation, is the requirement for an appropriate and dedicated light source. In addition, photochemical initiation in a therapeutic setting entails an application step followed by an irradiation step. The irradiation step usually requires nearly 1-minute of light exposure or longer to achieve high conversion. For applications requiring instantaneous application and gelation, redox initiation may be considered. Several redox pairs have been reported employing ascorbic acid [20], Tetramethylethylenediamine (TEMED) [21], or ferrous gluconate [22] as the reducing agent and persulfate salts ($S_2O_8^{2-}$) [20] hydrogen peroxide (H_2O_2) [22], or alkyl hydroperoxides as the oxidizing agent. The redox formulations can be prepared separately as two liquid parts. Upon mixing, the redox reaction generates free radicals which initiate crosslinking. When desired, gelation can be nearly instantaneous.

For many *in situ* hydrogel formulations, it may be possible to reach a gel point at a relatively low conversion of acrylate endgroups to poly(acrylate). Jarrett *et al*.[23] plotted compressive modulus of photo polymerized PEG diacrylate macromer as a function of %converted acrylate measured by ion chromatography. They found that a solid gel can be obtained at only 35% of acrylate conversion. However, polymerization to high conversion is strongly preferred due to the potential for hydrolytic liberation of toxic acrylic acid from unpolymerized acrylate endgroups in therapeutic environment. Furthermore, an *in situ* hydrogel composition with high conversion of acrylate endgroups will result in reproducible and consistent physical properties of the gel at the lowest possible macromer content. Despite the large number of studies utilizing hydrogels from PEG acrylate and methacrylate macromers, few

studies have addressed the comparative polymerization efficiency for various initiators or the effect of macromer structural features that influence polymerization efficiency.

2.2. Effects of Molecular Weight Distribution (MWD) on the Electrospinning Morphologies of Polymer Solutions

Electrospinning has attracted much attention in the recent decades as a simple and versatile processing technique for producing sub-micron to nano-scale fibers [24]. The sizes of these non-woven fibrous structures are one to several orders of magnitude thinner than those fabricated by conventional melt or solution spinning. Owing to the unique features such as very large specific surface-to-volume ratio and inter-connected porous structure, the electrospun fiber scaffolds can be adapted to be used in a broad range of applications such as sensor technology [25], catalysis [26], filtration [27], drug delivery systems [28] and protective clothing [29].

The solution viscosity of a homogeneous solution of a linear polymer can be described from the Huggins equation [31] as:

$$\eta_{sp}=[\eta]c+k_H([\eta]c)^2+\ldots \qquad (1)$$

where η_{sp} is the specific viscosity, $[\eta]$ is the intrinsic viscosity, c is the polymer concentration and k_H is the Huggins coefficient. The dimensionless product of the intrinsic viscosity and the concentration, $[\eta]c$, is referred to as Berry number (Be) [30]. The significance of the Berry number arises from the fact that, for a solution to have chain entanglements, $Be>1$.

The intrinsic viscosity, $[\eta]$, can be related to the molecular weight (M_w) of a linear polymer by the Mark-Houwink-Sakurada equation [32]:

$$[\eta]=KM_w^{\alpha} \qquad (2)$$

in which the constants K and α depend on the polymer, solvent and temperature [32]. Several regimes can be drawn for polymer solution based on the chain overlapping. The critical chain

overlap concentration, c^*, is the crossover concentration between the dilute and semi-dilute concentration regimes which can be expressed as $c^* \sim 1/[\eta]$. This criterion can be translated to what was discussed before regarding $Be>1$ as the limit of the chain entanglement. In dilute polymer solutions, the solution viscosity is proportional to the concentration. A scaling concept was established by Colby *et al.* [33] between solution viscosity and concentration, with a strong viscosity dependence on concentration ($\eta \sim c^{4.5}$).

Several studies have shown that the onset of fiber formation and the minimum concentration for uniform fiber formation vary with the polymer/solvent type, molecular weight (M_w) and molecular weight distribution (MWD) of the polymers. These studies allow the prediction of the polymer concentration for successful electrospinning. Koski *et al.* [34] used Berry number to discuss the minimum concentration needed to obtain stabilized fibrous structure. For aqueous poly(vinyl alcohol) (PVA) solutions investigated in their work, the minimum concentration corresponds to Berry number $[\eta]c>5$. Mckee *et al*. [35] determined the semi-dilute unentangled and semi-dilute entangled concentration regimes on the electrospinning process for a series of linear and branched (ethylene terephthalate-co-ethylene isophthalate) copolyesters. They concluded that the entanglement concentration (c_e) is the minimum concentration for electrospinning of beaded nano fibers, while 2-2.5 times c_e was the minimum concentration required for electrospinning uniform, defect-free fibers. Shenoy *et al.* [36] defined the entanglement number in solution $(n_e)_{soln}$ as the following equation:

$$(n_e)_{soln} = \frac{M_w c}{M_e} \qquad (3)$$

in which, M_w is average polymer molecular weight, M_e is the entanglement molecular weight, and c is the solution concentration. A correlation between chain entanglements and fiber formation was established based on experimental data obtained from electrospinning of several

polymer/solvent systems. Complete, stable fiber formation occurred at the number of entanglements $(n_e)_{soln} \geq 2$.

Gupta *et al.* [37] studied the scaling relation between viscosity and solution concentration of a series of seven linear poly(methyl methacrylate) (PMMA) homopolymers. The chain overlapping concentration, c^*, was determined and correlated with the solution regimes. Only polymer droplets were observed to form from electrospinning of solutions in the dilute concentration regime ($c/c^* < 1$), droplets and beaded fibers were observed in the semidilute unentangled regime ($1 < c/c^* < 3$), beaded as well as uniform fibers were observed in the semidilute entangled regime ($c/c^* > 3$) and uniform fiber formation was observed at $c/c^* \sim 6$ for all the narrow MWD polymers. They also compared the electrospinnability between relatively broad MWD PMMA and narrow MWD PMMA. Results showed that for the broad MWD polymers, uniform and bead-free fibers formation occurred at higher concentrations ($c/c^* = 9.7 \sim 10.1$) in contrast to the narrow MWD PMMAs' requirements of $c/c^* \sim 6$. Such difference, as explained by the authors, was due to the presence of the relatively small polymer chains that have small hydrodynamic volumes. Subsequently, during the process of plastic stretching, these small polymer chains acted as a weak link that caused a premature breakup of local "chain-chain coupling" within the jet, resulting in the formation of polymer droplets. As a result, higher concentration and viscosity were needed to attain sufficient entanglement density and to allow uniform fiber formation for the relatively broader MWD polymer when compared to the narrow MWD PMMA with an equivalent M_w.

It is well documented that viscosity of polymeric fluid is profoundly influenced by polymer MWD [38-43]. Gupta *et al*. [38] reported that the viscosity depended on the relaxation time necessitated by the individual components. In the solution of monodisperse polymer, all the

polymer chains had nearly the same hydrodynamic volume that resulted in a very sharp spectrum of relaxation times. In contrast, in a solution of polydisperse polymer, there was a wide distribution of hydrodynamic radii and relaxation times, in which larger components had slower relaxation times and smaller components had faster relaxation times. Ye and Sridhar [39] also observed a broader and gradual relaxation spectrum of a polydisperse solution than that of a monodisperse solution with M_n being constant. The broadening of the relaxation time spectrum lead to higher solution viscosity under extensional stress and increased shear rate dependence of the polymer solution. To describe the intrinsic viscosity of polydisperse polymer solutions, several models were developed in the format of power law dependence $[\eta]=(const.)M_t^a$, with M_t as the dominant molecular weight [40-43].

2.3. Effects of Additive on Electrospinning of Polymer Solutions

The main defects of electrospun fibers are considered to be beads and beaded fibers. During electrospinning processes, they can be widely observed distributed in the electrospun structures. The beaded structure can be eliminated by increasing the solution concentration. However, as a consequence, increase in fiber diameter is usually observed [44].

Several attempts have been made to eliminate beads by incorporating a small amount of additives in electrospinning polymer solutions including ionic salts [45], surfactants [46-50] and polyelectrolytes [51]. The additions of viscosity modifiers to electrospinning solutions were also reported [52,53]. Among these attempts, the interactions between surfactant and suitable polymers have attracted greater attention in the production of uniform nanofibers by electrospinning. A number of nonionic polymers have been electrospun with surfactants as a co-spinning agent to form uniform fibrous structures [46-50]. Various results were reported based on the nature of the surfactant. The three basic types of surfactant: nonionic, cationic and anionic were tested. Bhattarai *et al*. [46] studied the effects of a nonionic surfactant Triton X100^{TM} on the electrospinnability and structural uniformity of chitosan/poly(ethylene oxide) aqueous solutions. Results showed that the addition of the surfactant substantially improved the electrospun structure. However, bead-like structures were still seen embedded in the fibers. The effects of the same nonionic surfactant on electrospun structures of polyvinylpyrrolidone/water/ethanol solution were studied by Wang *et al*. [47]. Results showed that the addition of the surfactant greatly reduced the solution surface tension and substantially lowered the threshold voltage. A non-spinnable 48 wt.% PVP solution yielded sub-micron size uniform fibers on the order of 780 nm with the addition of surfactant. Kriegel *et al.* [48] evaluated the effects of a cationic surfactant, dodecyl trimethyl ammonium bromide (DTAB), on

the fiber formation of the chitosan-poly(ethylene oxide) (PEO) aqueous solutions. It was shown that the cationic surfactant had only minor effects on the fiber uniformity. Anionic surfactant such as sodium dodecyl sulfate (SDS) has been widely used in enhancing the electrospinnability of polymer solutions. Nagarajan *et al.* [49] successfully demonstrated the electrospun fiber formation of a gel forming, genetically engineered silk-elastin biopolymer by complexation with SDS. Wang *et al.* [50] showed that the addition of 1 wt.% SDS can dramatically decrease the fiber diameter of electrospun poly(vinyl alcohol) solutions. In these studies, however, researchers have been focusing on the effects of the addition of surfactant on polymer electrospinnability with surfactant concentration well above the surfactant critical micelle concentration (CMC). It was stated that the complexation between polymer and surfactant lead to low surface tension and high solution conductivity which favored the stability of the solution jet, thus allowing for formation of uniform fibrous structures. Overall, systematic studies had been rarely done to address the importance of molecular interactions between polymer and surfactant.

Polymer coil dimension change by molecular interactions with surfactant can be used to explain the electrospinning behavior. The conformation change of polyvinylpyrrolidone (PVP) binding with a series of surfactants was previously studied [54-58]. The binding mechanism changed depending on the different nature of surfactants. Molyneux *et al.* [54] observed the complexation between PVP and nonionic surfactant introduced coil contraction as a result of both hydrogen bonding and increase in polymer hydrophobicity, while cations had no effect on PVP chain dimensions due to the lack of binding. Interestingly, when binding with anionic surfactants, both contraction and expansion of PVP coils were observed [55,56]. It was reported that conformation changes depended on anionic surfactant concentration. When surfactant

concentration was above its critical micelle concentration (CMC), the polymer surfactant complex could be visualized by the 'necklace model' [57], as a series of spherical micelles with their surfaces covered by polymer segments and connected by strands of the same polymer molecules. The binding with micelles expanded PVP coil. However, at concentrations below CMC, contraction of the PVP coil occurred. By absorbing the surfactant anions, PVP essentially becomes a charged polyelectrolyte, the charges stretching the polymer chain just as they do in structural polyelectrolytes [58]. Studies showed that the anions had a salting-in effect on the amide groups (=N-CO), but a salting-out effect on the hydrocarbon backbone of the PVP chain [55]. As a result, the anions would attract the amide groups while repelling the rest of the molecule. The electrostatic repulsions lead to the rearrangement of the PVP coil into a smaller dimension. Thus, the anion bounded molecules tended to be salted-out from the solvent. With increasing anionic surfactant concentration, the charge density of PVP chain was anticipated to increase. The increasing repulsion between the charges could further disturb the formation of inter-molecular bonds between PVP coils. Overall, such intra-molecular interactions by the surfactant anions bind to the polymer segments lead to the shrinking of the polymer coil. However, it was reported that the charge repulsion depended on polymer chain length and the shrinking effect was also likely to have less influence on larger molecules than molecules with lower M_w [55].

Reference

1. J.A. Hubbell, “Biomaterials in Tissue Engineering,” *Nat. Biotechnol.*, 13(1995)565-76.
2. N.A. Peppas, “Hydrogels and Drug Delivery,” *Curr. Opinion Coll. Interfac. Sci.*, 2(1997)531-7.
3. S.R. Van Tomme, G. Storm, and W.E. Hennink, “*In Situ* Gelling Hydrogels for Pharmaceutical and Biomedical Applications,” *Int. J. Pharm.*, 355(2008)1-18.
4. A.S. Hoffman, “Hydrogels for Biomedical Applications,” *Adv. Drug Delivery Rev.*, 54(2002)3-12.

5. P.X. Ma, and J.H. Elisseeff, Ed. *Scaffolding in Tissue Engineering*, Boca Raton, FL, CRC press, 2005.
6. W.E. Hennink, and C.F. van Nostrum, "Novel Crosslinking Methods to Design Hydrogels," *Adv. Drug Delivery Rev.*, 54(2002)13–36.
7. J.B. Leach, and C.E. Schmidt, "Characterization of Protein Release from Photocrosslinkable Hyaluronic acid-Polyethylene Glycol Hydrogel Tissue Engineering Scaffolds," *Biomaterials*, 26(2005)125-35.
8. A.W. Watkins, and K.S. Anseth, "Investigation of Molecular Transport and Distributions in Poly(ethylene glycol) Hydrogels with Confocal Laser Scanning Microscopy," *Macromolecules*, 38(2005)1326-34.
9. V.A. Liu, and S.N. Bhatia, "Three-Dimensional Photopatterning of Hydrogels Containing Living Cells," *Biomed. Microdevices*, 4(2002)257-66.
10. A. Revzin, R.J. Russell, V. K. Yadavalli, W.-G. Koh, C. Deister, D.D. Hile, M.B. Mellott, and M.V. Pishko, "Fabrication of Poly(ethylene glycol) Hydrogel Microstructures Using Photolithography," *Langmuir*, 17(2001)5440-7.
11. S. He, M.J. Yaszemski, A.W. Yasko, P.S. Engel, A.G. Mikos, "Injectable Biodegradable Polymer Composites Based on Poly(propylene fumarate) Crosslinked with Poly(ethylene glycol)-Dimethacrylate," *Biomaterials*, 21(2000)2389-94.
12. F.M. Andreopoulos, E.J. Beckman, and A.J. Russell, "Light-induced Tailoring of PEG-Hydrogel Properties," *Biomaterials*, 19(1998)1343-52.
13. M. Micic, Y. Zheng, V. Moy, X.-H. Zhang, F.M. Andreopoulos, and R.M. Leblanc, "Comparative Studies of Surface Topography and Mechanical Properties of a New, Photo-switchable PEG-based Hydrogel," *Colloids Surf., B*, 27(2003)147-58.
14. A.S. Sawhney, C.P. Pathak, and J.A. Hubbell, "Bioerodible Hydrogels based on Photopolymerized Poly(ethylene glycol)-co-Poly(α-hydroxy acid) Diacrylate Macromers," *Macromolecules*, 26(1993)581-7.
15. J. Li, and W.J. Kao, "Synthesis of Polyethylene Glycol (PEG) Derivatives and PEGylated−Peptide Biopolymer Conjugates," *Biomacromolecules*, 4(2003)1055-67.
16. P.J. Martens, S.J. Bryant, and K.S. Anseth, "Tailoring the Degradation of Hydrogels Formed from Multivinyl Poly(ethylene glycol) and Poly(vinyl alcohol) Macromers for Cartilage Tissue Engineering," *Biomacromolecules*, 4(2003)283-92.
17. J.J. Sperinde, and L.G. Griffith, "Synthesis and Characterization of Enzymatically-Cross-Linked Poly(ethylene glycol) Hydrogels," *Macromolecules*, 30(1997)5255–64.
18. J.J. Sperinde, and L.G. Griffith, "Control and Prediction of Gelation Kinetics in Enzymatically Cross-Linked Poly(ethylene glycol) Hydrogels," *Macromolecules*, 33(2000)5476–80.
19. A.T. Metters, K.S. Anseth, and C.N. Bowman, "Fundamental Studies of a Novel, Biodegradable PEG-b-PLA Hydrogel," *Polymer*, 41(2000)3993–4004.
20. E. Behravesh, S.Jo,, K. Zygourakis, and A.G. Mikos, "Synthesis of *in Situ* Cross-Linkable Macroporous Biodegradable Poly(propylene fumarate-*co*-ethylene glycol) Hydrogels," *Biomacromolecules*, 3(2002)374-81.

21. W.E. Hennink, O. Franssen, W.N.E. van Dijk-Wolthuis, and H. Talsma, "Dextran Hydrogels for the Controlled Release of Proteins," *J. Controlled Release*, 48(1997)107-14.
22. D. Mawad, R. Odell, and L.A. Poole-Warren, "Network Structure and Macromolecular Drug Release from Poly(vinyl alcohol) Hydrogels Fabricated via Two Crosslinking Strategies," *Int. J. Pharm.*, 366(2009)31–7.
23. P. Jarrett, B.L. Cecily, L. Chan, M.P. Redmon, and A.J. Hickey, "Micelle Formation and Reaction Kinetics of a Bioabsorbable Polyethylene Glycol-oligolactide ABA Block Copolymer Hydrogel," *Colloids Surf., B*, 17(2000)11-21.
24. X. Wang, C. Drew, S.-H. Lee, K.J. Senecal, J. Kumar, and L.A. Samuelson, "Electrospinning Technology: a Novel Approach to Sensor Application," *J. Macromol. Sci. Part A Pure Appl. Chem.*, 39(2002)1251-8.
25. S. Madhugiri, B. Sun, P.G. Smirniotis, J.P. Ferraris, and K.J. Balkus Jr., "Electrospun Mesoporous Titanium Dioxide Fibers," *Microporous Mesoporous Mater.*, 69(2004)77-83.
26. R. Gopal, S. Kaura, Z. Ma, C. Chan, S. Ramakrishna, and T. Matsuura, "Electrospun Nanofibrous Filtration Membrane," *J. Membr. Sci.*, 281(2006)581-6.
27. E.D. Boland, J.A. Matthews, K.J. Pawlowski, D.G. Simpson, G.E. Wnek, and G.L. Bowlin, "Electrospinning Collagen and Elastin: Preliminary Vascular Tissue Engineering ," *Front. Bioscience*, 9(2004)1422-32.
28. J. Zeng, X. Xu, X. Chen, Q. Liang, X. Bian, L. Yang, and X. Jing, "Biodegradable Electrospun Fibers for Drug Delivery," *J. Controlled Release*, 92(2003)227-31.
29. P. Gibson, H. Schreuder-Gibson, and C. Pentheny, "Electrospinning Technology: Direct Application of Tailorable Ultrathin Membranes," *J. Ind. Text.*, 28(1998)63-72.
30. B.L. Hager, and G.C. Berry, "Moderately Concentrated Solutions of Polystyrene. I. Viscosity as a Function of Concentration, Temperature, and Molecular Weight," *J. Polym. Sci., Part B: Polym. Phys.*, 20(1982)911-928.
31. H. Morawetz, 1975. *"Macromolecules in Solution.*" Wiley, New York.
32. C. Tanford, 1961. "*Physical Chemistry of Macromolecules."* Wiley, New York.
33. R.H. Colby, L.J. Fetters, W.G. Funk, and W.W. Graessley, "Effects of Concentration and Thermodynamic Interaction on the Viscoelastic Properties of Polymer Solutions," *Macromolecules*, 24(1991)3873-82.
34. A. Koski, K. Yim, and S. Shivkumar, "Effect of Molecular Weight on Fibrous PVA Produced by Electrospinning," *Mater. Lett.*, 58(2004)493-7.
35. M.G. McKee, G.L. Wilkes, R.H. Colby, and T.E. Long, "Correlations of Solution Rheology with Electrospun Fiber Formation of Linear and Branched Polyesters," *Macromolecules*, 37(2004)1760-7.
36. S.L. Shenoy, W.D. Bates, H.L. Frisch, and G.E. Wnek, "Role of Chain Entanglements on Fiber Formation during Electrospinning of Polymer Solutions: Good solvent, Non-Specific Polymer–Polymer Interaction Limit," *Polymer*, 46(2005)3372-84.
37. P. Gupta, C. Elkins, T.E. Long, and G.L. Wilkes, "Electrospinning of Linear Homopolymers of Poly(methyl methacrylate): Exploring Relationships between Fiber Formation, Viscosity, Molecular Weight and Concentration in a Good Solvent," *Polymer*, 46(2005)4799-810.

38. M.J. Struglinski, and W.W. Graessley, "Effects of Polydispersity on the Linear Viscoelastic Properties of Entangled Polymers. 1. Experimental Observations for Binary Mixtures of Linear Polybutadiene," *Macromolecules*, 18(1985)2630-43.
39. X. Ye, and T. Sridhar, "Effects of the Polydispersity on Rheological Properties of Entangled Polystyrene Solutions," *Macromolecules,* 38(2005)3442-9.
40. M.M. Cross, "Polymer rheology: Influence of Molecular Weight and Polydispersity," *J. Appl. Polymer Sci.*, 13(1969)765-74.
41. J.A. Ressia, M.A. Villar, and E.M. Valles, "Influence of Polydispersity on the Viscoelastic Properties of Linear Polydimethylsiloxanes and Their Binary Blends," *Polymer*, 41(2000)6885-94.
42. A.Y. Malkin, N.K. Blinova, G.V. Vinogradov, M.P. Zabugina, O.Y. Sabsai, V.C. Shalganova, I.Y. Kirchevskaya, and V.P. Shatalov, "On Rheological Properties of Polydisperse Polymers," *Eur. Polym.J.*, 10(1974)445-51.
43. R.S. Anderssen, and D.W. Mead, "Theoretical Derivation of Molecular Weight Scaling for Rheological Parameters," *J. Non Newtonian Fluid Mech.*, 76(1998)299-306.
44. Y. Liu, J.-H. He, J.-Y. Yu, and H.-M. Zeng, "Preparation and Characterisation of Polyamide-Polyimide Prganoclay Nanocomposites," *Polym. Int.*, 57(2008)632-6.
45. T. Lin, H. Wang, H. Wang, and X. Wang, "The Charge Effect of Cationic Surfactants on the Elimination of Fibre Beads in the Electrospinning of Polystyrene." *Nanotechnology*, 15(2004)1375-81.
46. N. Bhattarai, D. Edmondson, O. Veiseh, F.A. Matsen, and M. Zhang, "Electrospun Chitosan-Based Nanofibers and Their Cellular Compatibility," *Biomaterials*, 26(2005)6176-84.
47. S.-Q. Wang, J.-H. He, and L. Xu, " Non-ionic Surfactants for Enhancing Electrospinnability and for the Preparation of Electrospun Nanofibers," *Polym. Int.*, 57(2008)1079-82.
48. C. Kriegel, K.M. Kit, D.J. McClements, and J. Weiss, "Influence of Surfactant Type and Concentration on Electrospinning of Chitosan–Poly(Ethylene Oxide) Blend Nanofibers," *Food Biophys.*, 4(2009)213-28.
49. R. Nagarajan, C. Drew, and C.M. Mello, "Polymer−Micelle Complex as an Aid to Electrospinning Nanofibers from Aqueous Solutions," *J. Phys. Chem. C*, 111(2007)16105-8.
50. M. Wang, H. Singh, T.A. Hatton, and G.C. Rutledge, "Field-Responsive Superparamagnetic Composite Nanofibers by Electrospinning," *Polymer*, 45(2004)5505-14.
51. T. Lin, J. Fang, H. Wang, T. Cheng, and X. Wang, "Gold-Nanoparticle-Based Miniaturized Laser-Induced Fluorescence Probe for Specific DNA Hybridization Detection: Studies on Size-Dependent Optical Properties," *Nanotechnology*, 17(2006)3718-23.
52. S. Talwar, J. Hinestroza, B. Pourdeyhimi, and S.A. Khan, "Associative Polymer Facilitated Electrospinning of Nanofibers," *Macromolecules*, 41(2008)4275-83.
53. M.T. Hunley, A. Harber, J.A. Orlicki, A.M. Rawlett, and T.E. Long, "Effect of Hyperbranched Surface-Migrating Additives on the Electrospinning Behavior of Poly(methyl methacrylate)," *Langmuir*, 24(2008)654-7.

54. P. Molyneux, and H.P. Frank, “The Interaction of Polyvinylpyrrolidone with Aromatic Compounds in Aqueous Solution. Part II. The Effect of the Interaction on the Molecular Size of the Polymer,” *J. Am. Chem. Soc.*, 83(1961)3175–80.
55. C.M. Klech, A.E. Cato III, and A.B. Suttle III, “Changes in Polyvinylpyrrolidone Coil Dimensions by Complexation with Organic Anions: Effect of Chain Length,” *Colloid Polym. Sci.*, 269(1991)643-9.
56. J. Eliassaf, F. Eriksson, and F.R. Eirich, “The Interaction of Poly(vinyl pyrrolidone) with Cosolutes,” *J. Polym. Sci.*, 47(1960)193-202.
57. S. Sen, D. Sukul, P. Dutta, and K. Bhattacharyya, “Fluorescence Anisotropy Decay in Polymer−Surfactant Aggregates,” *J. Phys. Chem. A*, 105(2001)7495-500.
58. M.N. Jones, “The Interaction of Sodium Dodecyl Sulfate with Polyethylene Oxide,” *J. Colloid Interface Sci.*, 23(1967)36-42.

CHAPTER 3: PUBLICATIONS

FREE RADICAL POLYMERIZATION OF PEG-DIACRYLATE MACROMERS: IMPACT OF MACROMER HYDROPHOBICITY AND INITIATOR CHEMISTRY ON POLYMERIZATION EFFICIENCY

(Submitted to *Acta Biomaterialia*)

Xiaoshu Dai[a], Xi Chen[b], Laura Yang[b], Sarah Foster[b], Arthur J. Coury[b], Thomas H. Jozefiak[b,*]

[a]Worcester Polytechnic Institute, Department of Material Science and Engineering, 100 Institute Road, Worcester, MA 01609

[b]Genzyme Corporation, Biomaterials Science and Engineering, 49 New York Avenue, Framingham, MA 01701

Abstract

A series of poly(ethylene glycol)-co-poly(lactate) diacrylate macromers was synthesized with variable PEG molecular weight (10 and 20 kDa) and lactate content (0-6 lactate per endgroup). These macromers were polymerized to form hydrogels by free radical polymerization using either redox or photochemical initiators. The extent of polymerization was monitored by compressive modulus of the resulting hydrogels and a quantitative determination of unreacted acrylate after exhaustive hydrolysis of the gel. Polymerization efficiency was found to depend on the lactate content of the macromer, with higher lactate macromers giving more efficient polymerization. For redox-initiated polymerization using ferrous gluconate/t-butyl hydroperoxide initiator, macromers containing approximately six lactate repeats per endgroup required lower concentrations of initiator to reach high conversion than lactate-free macromers. Photochemical polymerization with α, α-dimethoxy-α-phenylacetophenone (Irgacure 651®) was found to be less efficient than redox, requiring the addition of N-vinyl-2- pyrrolidone (NVP) as a co-monomer to achieve conversions comparable to redox polymerization. When conditions were

optimized to provide near complete conversion for all gels the presence of lactate repeat units in the hydrogel was generally found to reduce swelling and increase compressive modulus. Calculated values of molecular weight between crosslinks (Mc) and mesh size using Flory-Rehner theory showed that macromer molecular weight had the greatest impact on network structure of the gel.

Keywords

Poly(ethylene glycol), hydrogel, free radical, redox initiator, photoinitiator, polymerization, *in situ*

1. Introduction

In situ forming hydrogels represent a significant and versatile class of biomedical polymers. Many *in situ* forming hydrogel compositions have been developed in recent years for diverse applications such as hemostasis, tissue sealing, adhesion prevention, cell encapsulation, drug delivery and tissue engineering[1-7]. *In situ* forming hydrogel formulations are particularly advantageous for therapeutic modalities requiring injectable or minimally invasive application procedures. Cells and various therapeutic agents may be easily incorporated into liquid hydrogel formulations. Often *in situ* hydrogels are formed by the polymerization of water soluble telechelic polymers known as "macromers"[8, 9] . These water soluble macromers contain functionalities that enable polymerization by either condensation or free radical mechanisms. Optionally, macromers can contain chemical groups capable of degrading *in vivo*, thus tailoring the residence time of the hydrogel to meet the needs of the intended application.

Polyethylene glycol (PEG) is a synthetic polymer that has been used extensively in biomedical hydrogel systems due to its excellent biocompatibility. Many PEG derivatives capable of polymerization by free radical methods have been reported. Most commonly, these are

functionalized with acrylate and methacrylate groups at the chain ends [10-13], however fumarate[14], and other derivatives polymerizable via a free radical mechanism are known [15, 16]. In many of these cases, the polymerizable PEG macromers also include functionality allowing for degradation *in vivo* such as lactate, glycolate, glutarate or succinate[8, 17, 18].

Pioneering work in this area was performed by Hubbell and colleagues who used acrylate terminated PEG macromers to produce hydrogels crosslinked through a free radical polymerization mechanism[8, 19, 20]. Initiation of the hydrogel forming polymerization was demonstrated using either photochemical or redox methods. Subsequent studies by Hubbell and other laboratories largely employed photochemical initiation, owing to the convenient single-part formulation, and the exquisite control of the polymerization under mild and biocompatible conditions[21, 22] using light as an external stimulus.

Balancing the many advantages of *in situ* hydrogel formation by photochemical initiation, is the requirement for an appropriate and dedicated light source. In addition, photochemical initiation in a therapeutic setting entails an application step followed by an irradiation step. The irradiation step usually requires nearly 1-minute of light exposure or longer to achieve high conversion. For applications requiring instantaneous application and gelation, redox initiation may be preferred. Redox formulations are typically prepared using a 2-part liquid format. Upon mixing, the redox reaction generates free radicals which initiate polymerization. For optimized formulations, gelation can be nearly instantaneous. Free radical polymerization of macromers for *in situ* hydrogel formation has been reported using common redox initiators such as persulfate/TEMED, ferrous gluconate/HOOH, and others[23-27].

For many *in situ* hydrogel formulations it may be possible to reach a gel point at relatively low conversion of acrylate endgroups to poly(acrylate), however polymerization to high conversion is strongly preferred. An *in situ* hydrogel composition with high conversion of acrylate endgroups will result in reproducible and consistent gel physical properties as a function of macromer content. Also, the potential for hydrolytic liberation of toxic acrylic acid from unpolymerized acrylate endgroups in the therapeutic environment can be minimized. Despite the large number of studies employing hydrogels from PEG acrylate and methacrylate macromers, few studies have addressed comparative polymerization efficiency for various initiators and the effect of macromer structural features on polymerization efficiency. In this report, we examine the efficiency of polymerization for several simple PEG diacrylate macromers comparing redox and photochemical initiation processes. In addition, we illustrate the importance of hydrophobic modification of macromer structures on the efficiency of polymerization. For our model system, efforts have been made to optimize the polymerization conditions and compare the physical properties of the resulting hydrogels at similarly high acrylate conversion. To characterize network structure the average molecular weight between crosslinks and the mesh size were calculated from hydrogel swell data.

2. Materials and methods

2.1. Materials

Polyethylene glycol (PEG) with molecular weights of 10,000 g/mol and 20,000 g/mol, Tin(II) 2-ethylhexanoate (stannous octoate), DL-lactide, triethylamine (TEA), acryloyl chloride (AC), hydroquinone (HQ), the redox initiator ferrous gluconate dihydrate (Fe(Glu)2H2O) and tert-butyl hydroperoxide (tBHP) as well as the photo initiator 2,2-dimethoxy-1,2-diphenylethan-1-one

(Ciba Irgacure 651®), N-vinyl pyrrolidone (NVP) and N-methyl-2-pyrrolidone (NMP) were all purchased from Sigma-Aldrich (Milwaukee, WI). Toluene, hexane and isopropyl alcohol (IPA) were purchased from J.T.Baker (Phillipsburg, NJ). Phosphate-buffered Saline (PBS) was purchase from Gibco (North Andover, MA). All chemicals used were of reagent grade and were used without further purification.

2.2. Macromer synthesis

All modified PEG macromers were synthesized using a one-pot procedure in toluene. The synthesis of 20K PEG diacrylate modified with 6 lactate groups per chain end is briefly described below. Linear polyethylene glycol 20 kDa (100 g, 10 meq in hydroxyl endgroups) was dissolved in 1300 mL of toluene under dry nitrogen atmosphere in a 2-liter round bottom flask fitted with magnetic stirring. Azeotropic distillation was performed until a total amount of 1000 mL of toluene was removed. The resulting solution (approximately 30% wt./vol.) was then allowed to cool to 80°C. A toluene solution of stannous octoate (40 mg in 2 ml) was added followed by the addition of DL-lactide solid (10.8g, 75 mmol). The ring-opening polymerization reaction was performed at 112-115 °C for 24 hr under nitrogen atmosphere with light reflux. An additional 1000 mL of toluene were then added to the solution and it was allowed to cool to 45°C. Triethylamine (5.2 mL, 37.3 mmol) was then added in one portion followed by the dropwise addition of acryloyl chloride (2.50 ml, 30.9 mmol) at a rate maintaining reaction temperature between 45 -50°C. The reaction mixture was stirred at 45°C for two hours under nitrogen atmosphere and then vacuum filtered through a coarse glass frit removing TEA-hydrochloride salt. The filtrate was collected and passed through a short column of alumina (200 g) in toluene providing a clear, colorless solution. A hydroquinone/acetone solution (30 mg/5

ml) was added to the filtrate as a stabilizer. This solution was then slowly poured in to a 2000 mL of hexane with moderate magnetic stirring. A white precipitate was immediately evident. After the addition, the mixture was allowed to stir for 30 min. The final product was collected by vacuum filtration through a Büchner funnel equipped with a medium glass frit and dried under vacuum at ambient temperature for at least 12 hours. A dry white powder (84 g, 80% of theoretical yield) was obtained. The macromer was stored at -20°C in an amber bottle under dry argon.

2.3. Macromer characterization

Macromer molecular weight (M_w) was determined using size exclusion chromatography (SEC). A gel permeation chromatograph with a TSK G4000SW column was used. The mobile phase was 50/50 IPA/water (isocratic) and the flow rate was 0.4 mL/min. A refractive index detector was used for determination of mass concentration and a Wyatt multi-angle-laser-light-scattering (DAWN EOS MALLS) detector was used for precise M_w determination.

Macromer composition was verified using proton nuclear magnetic resonance (^{1}H NMR) spectroscopy. Spectra were measured using Bruker AVANCE II, 400MHz instrument. Samples were prepared in deuterated chloroform ($CDCl_3$) with tetramethylsilane (TMS) as an internal standard. NMR signals corresponding to the PEG methylene protons were observed at δ = 3.4-3.9 ppm. NMR signals at δ = 4.2 - 4.3 ppm were assigned to the terminal PEG methylene protons. Signals at δ = 5.0 - 5.25 ppm and δ = 1.4 - 1.6 ppm represent the lactate methine and methyl protons respectively. Acrylate proton signals were seen at δ = 5.9, 6.2 and 6.4 ppm. The number of lactate and acrylate functional groups per chain end group was determined from the

ratio of the integrated peak areas for the appropriate NMR signal using a conversion factor derived from the total PEG integral and the determined molecular weight of the PEG starting material from SEC-MALLS. Thus, a 10kDa PEG macromer terminated by 6 lactate repeats per chain end and end capped with acrylate units was designated $10K(L_6A)_2$.

CMC values for macromer solutions were determined using Static Light Scattering (SLS). SLS measurements were performed with a DAWN-DSP Laser Photometer (Wyatt Technology Inc) in batch mode. A He-Ne laser with 658nm (Spectra-Physics 124B) light source was used. The instrument was calibrated with pure toluene by taking the Rayleigh ratio at room temperature (21 ^{o}C) as 1.406×10^{-5} cm^{-1}. Samples were prepared at a broad range of concentrations from 0.005% to 5%. The solutions were filtered through PALL Acrodisc PF 0.8/0.2μm syringe filters (PALL Corporation). The solutions were maintained at 21.0 ± 0.1°C during the scattering experiments. The photometer provided a detector response in mV that is correlated to the amount of light scattered by the sample at an angle of 90°. Detector response readings were plotted vs. macromer concentration. In the portion of the plot where detector response increased linearly with concentration, this linear relationship was extrapolated to zero to determine the CMC value.

2.4. Macromer polymerization

Macromers were formulated by dissolution in deionized (DI) water at ambient temperature (21.0 °C) to achieve a final concentration of 10% (wt./vol.). For redox polymerization, concentrated aqueous solutions of Fe(Glu)2H2O and tBHP were prepared and separately added to two 10% macromer aqueous solutions providing the desired molar concentrations of initiator. The reducing and the oxidizing precursor solutions were then loaded into separate sides of a mini-

dual syringe (4B19 – 2 mL x 2 mL, 1:1 Ratio, Plas-Pak Industries, Inc. Norwich, TC) equipped with a Micro-mixer (3mm x 8 Element needle tip, Plas-Pak Industries, Inc. Norwich, TC). The plunger was depressed to dispense 0.25 mL of the mixed formulation into a cylindrical Teflon mold with a diameter of 0.8 cm. Polymerization took place within seconds, and the hydrogel could easily be removed from the Teflon mold for analysis. For photopolymerization, a photoinitiator stock solution was prepared by dissolving desired amounts of Irgacure 651® in either NVP or NMP. Calculated amounts of the photoinitiator solution were then added to a 10% macromer aqueous solution. A 0.25 mL volume of the precursor was pipetted into the same Teflon mold used for redox polymerization. The filled mold was exposed to a UV light source (365nm, 50 mW/cm^2) for 40 seconds.

2.5. Hydrogel characterization

Uniaxial compression experiments were performed at 37°C on the cylindrical gel samples prepared as described above (0.6 cm diameter, 0.5 cm height). A dynamic mechanical analysis instrument (Model Q800, TA Instruments, New Castle, DE) with a compression clamp was ussed. The sample was loaded on the clamp stage under a pre-load force of 0.001N. An isothermal condition at 37^{o} C was then applied for 1 min. With a force ramp rate of 0.5N/min, the compression force was loaded up to 5.0 N. The compressive modulus was calculated as the slope of the initial linear portion of the stress-strain curve (strain 5%-15%). Three samples were tested for each polymerization condition. Averages and standard deviations were reported.

Swelling studies were performed to determine how much water a polymerized hydrogel would take up in a 24 hour period. The wet weight of the as-polymerized sample was measured as m_0.

Three samples from each formulation were weighed and incubated in PBS at 37° C for 24 hours. After incubation, the swollen samples were removed from solution, carefully blotted to remove external surface droplets, and weighed again to obtain m_{24}. The percentage weight gain was calculated as

$$\%swelling = \frac{m_{24} - m_0}{m_0} \times 100 \qquad (1)$$

Macromer polymerization was quantified by the determination of unreacted acrylic acid liberated from exhaustive hydrolysis of the hydrogels. Ion Chromatography (Dionex ICS3000 with eluent generator and conductivity detector equipped with Dionex AS11-HC column, Dionex AG11-HC guard column and ASRS300 suppressor) was used to quantify acrylic acid as well as lactic acid after hydrolysis. Approximately 10 mg of macromer solid or 100 mg of a 10% gel were hydrolyzed in 2 mL of 0.2 N NaOH at 80°C for one hour. After cooling to room temperature, the solution was diluted with water to achieve a final concentration of 25 mL. Calibration curves for acrylic acid and lactic acid aqueous solutions were obtained to show linear response in the concentration range of interest (20 to 500 μM for lactic acid and 10 to 250 μM for acrylic acid with limits of detection for both lactic acid and acrylic acid are around 1μM with 10 μL). Based on the peak areas for lactic acid and acrylic acid, the concentrations (μM) of lactic and acrylic acid were determined using the calibration curves.

The number average molecular weight between crosslinks, $\overline{M_c}$, was calculated using the Flory-Rehner equation as modified by Peppas and Merrill[5, 28] for hydrogels prepared in water.

$$\frac{1}{\overline{M_c}} = \frac{2}{M_n} - \frac{\bar{\upsilon} / V_1 \left[\ln\left(1 - \upsilon_{2,s}\right) + \upsilon_{2,s} + \chi \upsilon_{2,s}^2\right]}{\upsilon_{2,r}\left[\left(\upsilon_{2,s} / \upsilon_{2,r}\right)^{1/3} - 0.5\left(\upsilon_{2,s} / \upsilon_{2,r}\right)\right]} \qquad (2)$$

where M_n is the number-average molecular weight of the uncrosslinked polymer (the molecular weight of the macromer), $\bar{\upsilon}$ is the specific volume of bulk amorphous PEG (0.893 cm^3/g), and V_1 is the molar volume of water (18cm^3/mol). A value of 0.426 was used for the Flory-Huggins polymer-solvent interaction parameter χ (PEG/water)[29], and this was assumed constant for all gels[30]. The parameters υ_{2r} and υ_{2s} are respectively the volume fraction of polymer in the relaxed gel and swollen gel. These are defined in the following expressions:

$$\upsilon_P = \frac{W_P}{\rho_P}, \quad \upsilon_{2,r} = \frac{\upsilon_P}{\upsilon_r}, \quad \upsilon_{2,s} = \frac{\upsilon_P}{\upsilon_s} \qquad (3)$$

Where υ_P is the bulk polymer volume, W_P is the weight of the dry polymer, ρ_P is the bulk density of the polymer, υ_r is the volume of the gel as initially prepared and υ_s is the volume of the swollen gel calculated from υ_r and our measured %swell value.

The mesh size was calculated by first computing the end-to-end distance of the solvent-free state, r_0^{-2} described by Canal and Peppas[31]:

$$\left(r_0^{-2}\right)^{1/2} = l\left(2\frac{M_c}{M_r}\right)^{1/2} C_n^{1/2} \qquad (4)$$

in which l is the average bond length (typically 1.50Å is used for PEG), M_r is the molecular weight of the PEG repeat unit (44 $g \cdot mol^{-1}$), C_n is the characteristic ratio for PEG (a value of 4.0 value was used [32]).

The mesh size, ξ, can then be calculated by equation 5.

$$\xi = \left(r_0^{-2}\right)^{1/2} \upsilon_{2,s}^{-1/3} \qquad (5)$$

3. Results

3.1. Macromer synthesis and characterization

Macromers were synthesized from the modification of 10K and 20K linear PEG diols in a two-step, one-pot procedure in toluene. The number of lactate and acrylate functional groups incorporated in the macromer structure was estimated by proton NMR spectroscopy and quantified by the determination of lactic acid and acrylic acid in macromer hydrolysate using IC. The estimated of macromer composition from the integration of NMR signals were consistent with the estimated IC results (Table 1). SEC-MALLS analysis was performed using an IPA/water eluent in order to eliminate artifacts due to macromer aggregation in aqueous media. Weight-average molecular weight (Mw) values are shown in Table 1. The molecular weight of the PEG diol starting material and the PEG macromers are consistent with expectations and the SEC chromatograms are nearly super imposable, suggesting no significant change in polydispersity between the initial PEG diols and the macromers derived from them.

It is known that the PEG chains modified at their chain ends with hydrophobic groups form micellar structures in aqueous solution[33-35]. Static light scattering (SLS) was used to probe the aqueous solution aggregation of our macromers as well as unmodified PEG. The mean intensities of the scattered light as a function of the solution concentration are plotted in Figure 2. The lactate-containing macromers were shown to have very low CMC values: 10KPEG($L_{6.2}A_{0.95}$)$_2$ CMC = 0.22% w/v, 20KPEG($L_{5.8}A_{0.95}$)$_2$ CMC = 0.13% w/v. However, aggregation of lactate-free PEG diacrylates was not discernable using this method. For these macromers the low scattering intensity observed at high concentrations was nearly identical to that of the unmodified PEG diols (Figure 2).

3.2. Macromer polymerization with redox initiation

Macromers were formulated in a 2-part liquid format including Fe(Glu)2H2O in part-A and tBHP in part-B. Both solutions contained 10% macromer. Rapid formation of gel was observed upon mixing the two solutions. A series of gels was prepared at constant tBHP concentration (1.94 mM in part-B solution) varying the concentration of Fe(Glu)2H2O in the part-A solution. Dynamic mechanical analysis of these gels showed a steady increase of compressive modulus with increasing Fe(Glu)2H2O concentration leading to a plateau value (Figure 3; a1-d1). Repeating this experiment at constant Fe(Glu)2H2O concentration (6.20 mM in part-A) and varying the concentration of tBHP provided a similar result (Figure 3; a2-d2). The lactate-containing macromers require lower initiator concentrations to reach the plateau region.

From this analysis, optimal concentrations for both Fe(Glu)2H2O and tBHP were used to formulate macromers and prepare gels for a determination of acrylate conversion by IC and to study swelling behavior. As seen in Table 2, optimized gels provided compressive modulus values consistent with the initial optimization experiment. In general, under these optimized conditions residual unreacted acrylate was found by IC to be very low. Swelling at 37°C for 24 hours showed that although compressive modulus values were similar for gels with or without lactate, the lactate-containing gels swelled considerably less (2-3X) than the lactate-free gels. Also the 20K PEG gels swelled considerably more (2-3X) than the 10K PEG gels.

3.3. Macromer polymerization with photochemical initiation

Macromers were formulated with Irgacure 651® dissolved in the inert solvent N-methyl-pyrrolidone (NMP) providing homogeneous solutions that could be polymerized to form gels

after UV irradiation. An experiment to determine optimal Irgacure concentrations was performed using a constant 40 second illumination time. This experiment showed that the formulations of lactate-modified macromers polymerized to form hydrogels with compressive modulus increasing with greater Irgacure concentrations, but these gels did not achieve comparable modulus values as high as the redox polymerized gels. Furthermore, the lactate-free macromer formulations formed no gels under these conditions (Figure 4; a1-d1).

This experiment was repeated using formulations in which Irgacure had been dissolved in N-vinyl-2- pyrrolidone (NVP), a reactive monomer for free radical polymerization. NVP concentrations were then adjusted so all formulations contained the same concentration (13.5 mM). By substituting NVP in place of NMP, all formulations gave gels including those for the lactate-free macromers (Figure 4; a2-d2). Formulations with lactate-modified macromers gave gels with higher compressive modulus values, similar to those obtained using redox initiators.

Dependence on NVP was then investigated at a constant Irgacure concentration (1.76 mM). Under these conditions, lactate-modified macromers were found to achieve compressive modulus plateau values similar to those seen for comparable redox gels when NVP concentration reached the 9-13 mM range for 10K macromers and 4.5-9 mM range for 20K macromers, as shown in Figure 5 (series b and d). However, for lactate-free macromers, compressive modulus values at these concentrations of NVP were still low and continued to increase as NVP concentration was raised even higher (see Figure 5; series a and c).

Gel samples were then prepared using photochemical initiation with using conditions judged to be optimal. As seen in Table 3, modulus values for photopolymerized gels with NVP were comparable to the redox polymerized gels. However, lactate-free gels gave lower acrylate conversion than the comparable redox gels. These lactate-free hydrogels were found to swell

less than comparable redox gels despite their lower acrylate conversion; however due to the large amount of NVP co-monomer used, these gels are expected to have properties different from the NVP-free, redox-initiated gels. In this regard we find that incorporation of NVP in the gel results in a firmer, and lower swelling network.

3.4. Average molecular weight between crosslinks ($\overline{M}_c$) and mesh size (ξ) calculation

Hydrogel swell data were used to calculate gel network properties using the well known equations 2 and 5. We measured swell (37°C, PBS) for the hydrogels of this study at 24 hours and calculated the values for average molecular weight between crosslinks ($\overline{M}_c$) and mesh size (ξ) shown in Table 4. For redox initiated polymerization, a larger mesh size was calculated for hydrogels derived from the 20kDa macromers relative to the 10kDa macromers. Also, the lactate-free macromers gave gels with slightly larger mesh size than the lactate-modified macromer of the same molecular weight. Similar trends were seen for the gels from photo initiated polymerization, but the incorporation of NVP in the gel structure minimized the influence of lactate content on mesh size. Similar values have been reported by Cruise *et al* [36] who determined average molecular weight between crosslinks and mesh size for a 10% 20K PEG diacrylate gel polymerized using an interfacial procedure and visible-light photochemical initiation (ethyl eosin/triethanolamine).

4. Discussion

4.1 Macromer Synthesis and Characterization

Synthesis of modified PEG macromers in a 1-pot procedure in toluene was convenient and relatively efficient. It was found that with this procedure that a 2.5X molar excess of lactide was

required over the amount of modification targeted. Effective acrylation was observed using 2X molar excess of acryloyl chloride. Purification was achieved by filtration through alumina rather than multiple dissolution-reprecipitation cycles. The alumina filtration method has been reported for the purification of other modified PEG materials[37, 38]and was effective in our hands as demonstrated by NMR spectra free of peaks other than those expected for the desired product. Material yields were typically 80% or higher. Though the compositional analysis from NMR was approximate, this method agreed well with the true macromer composition determined through exhaustive hydrolysis of macromer in NaOH solution followed by lactate and acrylate determination by ion chromatography.

When examined in dilute aqueous solution using static light scattering, none of the macromers in this study scattered light at concentrations below 0.1 wt%. For the lactate-free macromers, a small amount of scattering was observed at concentrations in the 0.5 - 1 wt% range, however we found that unmodified PEG provided a similar scattering result. An equivalent result was found for lightly lactate modified macromers 10KPEG($L_2A)_2$ and 20KPEG($L_2A)_2$ (data not shown). In contrast, a significant amount of scattering at low concentration was observed for the PEG($L_6A)_2$ macromers. This dramatic difference supports the conclusion that the lactate-free macromers are well solvated in water (similar to unmodified PEG), but the L6 macromers form structured solutions (micelles or solution aggregates) that strongly scatter light at very low concentrations. The low CMC values (0.22%w/v for 10KPEG($L_6A)_2$ and 0.13wt%w/v for 20KPEG($L_6A)_2$) are consistent with those reported for other hydrophobically modified PEG derivatives[39].

4.2 Macromer polymerization with redox initiation

When formulated with Fe(Glu)2H2O and tBHP, all macromers in this study formed gels within seconds of mixing. Variation of initiator concentration using compressive modulus as a measure of gel formation revealed that above a critical initiator concentration a plateau modulus value was achieved for all macromers. This result suggests that a maximum degree of crosslinking had been reached. For both 10K and 20K macromers, this plateau modus value was reached at significantly lower initiator concentration for the lactate-containing macromers than the lactate-free macromers. Subsequent IC analysis of unreacted acrylate in hydrogels made with an optimized redox formulation confirmed that indeed only very small levels of acrylic acid could be detected. The higher polymerization efficiency observed for the lactate-containing macromer solutions is attributed to the increased local concentration of acrylate groups within hydrophobic environments of the structured solutions, allowing a more efficient propagation reaction in free radical polymerization[34, 35].

4.3 Macromer polymerization with photochemical initiation

In the absence of NVP as an accelerating co-monomer, the crosslinking efficiency observed for photopolymerization with Irgacure 651® was surprisingly poor relative to the redox initiated formulations. The water-soluble photoinitiator Irgacure 2959, frequently reported for PEG diacrylate photopolymerization[22], also provided low modulus gels and required long irradiation times in the absence of NVP (data not shown). Literature reports of PEG-acrylate photopolymerization most often include NVP in the formulation, and in our study we find this co-monomer to be critical for efficient photopolymerization. Published reports [40-42] have proposed that a dramatic improvement of photopolymerization efficiency for acrylate monomers in the presence of NVP is derived from a 1:1 NVP/acrylate charge transfer complex as an active

intermediate in the polymerization reaction. In our study, 10% formulations of 10K and 20K macromers containing 20 meq and 10 meq acrylate respectively showed a maximum benefit of added NVP when co-monomer equivalents rose to levels matching the number of acrylate equivalents. Here again we found that lactate-modified macromers provided gels with higher compressive modulus at lower Irgacure/NVP concentrations relative to lactate-free macromers.

4.4 Average molecular weight between crosslinks ($\overline{M_c}$) and mesh size (ξ) calculation

Typical hydrogels obtained by chemical crosslinking or irradiation yield structures with crosslinks randomly distributed throughout the network. In contrast, the macromers used in our study result in a unique gel structure comprised of a series of hydrophobic poly(acrylate) domains interconnected by a number of hydrophilic PEG chains. The length of PEG chains is known from the initial macromer, but the degree of polymerization of the hydrophobic poly(acrylate) chains has not been measured in our study and is known to be influenced by initiation conditions[43, 44]. The molecular weight between crosslinks (Mc) will be influenced by both the PEG molecular weight and the degree of acrylate polymerization. Interestingly, the theoretical calculation of Mc using hydrogel swelling data gives values that are only 10-20% of the known PEG molecular weight. A direct comparison of the network structure of hydrogels crosslinked by redox and by photoinitiators is difficult due to differences in chemical composition brought about by incorporation of NVP into the photopolymerized gel structure.

Conclusions

Several PEG diacrylate macromers were formulated with redox or photochemical initiators to provide hydrogels. Experimental results suggested hydrophobic modification is required to

achieve low concentration aggregation and high polymerization efficiency. Photochemical polymerization is difficult to achieve in the absence of NVP as an accelerating co-monomer, particularly for macromers that lack hydrophobic modification. Swell data showed that when optimized to similarly high conversion, hydrogel network structure was most strongly influenced by macromer hydrophobicity and molecular weight.

Figure Captions

Figure 1. Molecular structure and proton NMR spectrum for the 20K PEG-co-lactate-acrylate block copolymer 20K(L6A)2.

Figure 2. Static Light Scattering(SLS) intensity as a function solution concentration for (a)10K and (d)20K unmodified PEG-diol, (b)10K and (e)20K (L0A)2, (c)10K and (f)20K (L6A)2 macromers.

Figure 3. Compressive moduli for redox crosslinked 10% macromer hydrogels: (a)10K(L0A)2, (b)10K(L6A)2, (c) 20K(L0A)2, and (d)20K(L6A)2. Condition 1: variable [Fe(Glu)2] with [tBHP] = 1.94mM. Condition 2: variable [tBHP] with [Fe(Glu)2] = 6.20mM.

Figure 4. Compressive moduli for photopolymerized 10% macromer hydrogels: (a) 10K(L0A)2, (b) 10K(L6A)2, (c) 20K(L0A)2, and (d)20K(L6A)2. Condition 1: variable [Irgacure] with [N-methylpyrrolidone] = 13.5 mM. Condition 2: variable [Irgacure] with [NVP] = 13.5 mM.

Figure 5 Compressive moduli of photopolymerized 10% macromer hydrogels: (a) 10K(L0A)2, (b) 10K(L6A)2, (c) 20K(L0A)2, and (d)20K(L6A)2 as a function of [NVP] with [Irgacure] = 1.76 mM

Table 1. Macromer composition and molecular weight.

	NMR	IC	M_w (kDa)
10K Linear	$(L_0A_{0.95})_2$	$(L_0A_{1.0})_2$	11.40
	$(L_{6.2}A_{0.90})_2$	$(L_{6.3}A_{1.0})_2$	12.40
20K Linear	$(L_0A_{0.88})_2$	$(L_0A_{0.9})_2$	21.78
	$(L_{5.8}A_{0.84})_2$	$(L_{5.9}A_{0.8})_2$	23.70

Table 2. Optimized formulations for redox polymerized 10% macromer hydrogels: compressive modulus, 24 hour swell, and residual acrylate.

Gel sample Information	Initiator Concentration (mM)		Max. Compressive Modulus (-kPa)	% Swell	% Residual Acrylate
	[Fe(Glu)2]	[tBHP]			
$10K(L_0A)_2$	6.20	1.94	68.2 ± 0.8	53 ± 6	2.8 ± 2.0
$10K(L_6A)_2$	4.13	1.36	94.0 ± 2.1	19 ± 1	1.9 ± 0.1
$20K(L_0A)_2$	6.20	1.94	42.9 ± 1.4	133 ± 3	1.4 ± 1.0
$20K(L_6A)_2$	4.13	1.36	55.0 ± 0.7	74 ±0.3	1.8 ± 1.0

Table 3. Formulations for photopolymerized 10% macromer hydrogels: compressive modulus, 24 hour swell, and residual acrylate.

Macromer (10 wt%)	[Irgacure] (mM)	[NVP] (mM)	Max. Compressive Modulus (-kPa)	% Swell	% Residual Acrylate
$10K(L_0A)_2$	17.6	18.0	76.3 ± 0.3	23 ± 1	8.1 ± 0.1
$10K(L_6A)_2$	17.6	13.5	91.8 ± 0.7	18 ± 0.5	0.5 ± 0.4
$20K(L_0A)_2$	17.6	18.0	47.8 ± 0.3	79 ± 1	4.4 ± 0.8
$20K(L_6A)_2$	17.6	13.5	55.1±0.8	84 ± 5	0.17 ± 0.3

Table 4. Molecular weight between crosslinks ($\overline{M_c}$) and mesh size (ξ) of hydrogels crosslinked by redox and photo initiation methods.

Macromer (10 wt%)	Crosslinking Conditions		% Swell	$\overline{M_c}$ ($g \cdot mol^{-1}$)	Mesh Size (ξ) (Å)
$10K(L_0A)_2$	[Fe(Glu)2]=6.20 mM	[tBHP]=1.94mM	53 ± 6	1462 ± 78	63 ± 3
	[Irgacure]=1.76 mM	[NVP]=18.0 mM	23 ± 1	1067 ± 15	50 ± 1
$10K(L_6A)_2$	[Fe(Glu)2]=4.13 mM	[tBHP]=1.36 mM	19 ± 1	1008 ± 25	48 ± 1
	[Irgacure]=1.76 mM	[NVP]=13.5 mM	18 ± 0.5	1004 ± 6	48 ± 0
$20K(L_0A)_2$	[Fe(Glu)2]=6.20 mM	[tBHP]=1.94 mM	133 ± 3	3264 ± 66	109 ± 2
	[Irgacure]=1.76 mM	[NVP]=18.0 mM	79 ± 1	2206 ± 22	82 ± 1
$20K(L_6A)_2$	[Fe(Glu)2]=4.13 mM	[tBHP]=1.36 mM	74 ±0.3	2101 ± 5	79 ± 0
	[Irgacure]=1.76 mM	[NVP]=13.5 mM	84 ± 5	2301 ± 93	84 ± 3

References

[1] Hatefi A, Amsden B, editors. Biodegradable injectable in situ forming drug delivery systems. Netherlands, 2002.

[2] He C, Kim SW, Lee DS. In situ gelling stimuli-sensitive block copolymer hydrogels for drug delivery. J Controlled Release 2008;127:189-207.

[3] Hoffman AS. Hydrogels for biomedical applications. Adv Drug Deliv Rev 2002;54:3-12.

[4] Klouda L, Mikos AG. Thermoresponsive hydrogels in biomedical applications. Eur J Pharm Biopharm 2008;68:34-45.

[5] Peppas NA, Hilt JZ, Khademhosseini A, Langer R. Hydrogels in biology and medicine: from molecular principles to bionanotechnology. Adv Mater (Weinheim, Ger) 2006;18:1345-60.

[6] Van Tomme SR, Storm G, Hennink WE. In situ gelling hydrogels for pharmaceutical and biomedical applications. Int J Pharm 2008;355:1-18.

[7] Nicodemus GD, Bryant SJ. Cell Encapsulation in Biodegradable Hydrogels for Tissue Engineering Applications. Tissue Eng, Part B 2008;14:149-65.

[8] Sawhney AS, Pathak CP, Hubbell JA. Bioerodible hydrogels based on photopolymerized poly(ethylene glycol)-co-poly(Î±-hydroxy acid) diacrylate macromers. Macromolecules 1993;26:581-7.

[9] Metters A, Hubbell J. Network formation and degradation behavior of hydrogels formed by Michael-type addition reactions. Biomacromolecules 2005;6:290-301.

[10] Bencherif SA, Srinivasan A, Sheehan JA, Walker LM, Gayathri C, Gil R, et al. End-group effects on the properties of PEG-co-PGA hydrogels. Acta Biomater 2009;5:1872-83.

[11] Anseth KS, Kline LM, Walker TA, Anderson KJ, Bowman CN. Reaction Kinetics and Volume Relaxation during Polymerizations of Multiethylene Glycol Dimethacrylates. Macromolecules 1995;28:2491-9.

[12] Leach JB, Schmidt CE. Characterization of protein release from photocrosslinkable hyaluronic acid-polyethylene glycol hydrogel tissue engineering scaffolds. Biomaterials 2005;26:125-35.

[13] Revzin A, Russell RJ, Yadavalli VK, Koh WG, Deister C, Hile DD, et al. Fabrication of poly(ethylene glycol) hydrogel microstructures using photolithography. Langmuir 2001;17:5440-7.

[14] He S, Yaszemski MJ, Yasko AW, Engel PS, Mikos AG, editors. Injectable biodegradable polymer composites based on poly(propylene fumarate) crosslinked with poly(ethylene glycol)-dimethacrylate. England, 2000.

[15] Andreopoulos FM, Beckman EJ, Russell AJ. Light-induced tailoring of PEG-hydrogel properties. Biomaterials 1998;19:1343-52.

[16] Micic M, Zheng Y, Moy V, Zhang X-H, Andreopoulos FM, Leblanc RM. Comparative studies of surface topography and mechanical properties of a new, photo-switchable PEG-based hydrogel. Colloids Surf, B 2003;27:147-58.

[17] Martens PJ, Bryant SJ, Anseth KS. Tailoring the Degradation of Hydrogels Formed from Multivinyl Poly(ethylene glycol) and Poly(vinyl alcohol) Macromers for Cartilage Tissue Engineering. Biomacromolecules 2003;4:283-92.

[18] Li J, Kao WJ. Synthesis of Polyethylene Glycol (PEG) Derivatives and PEGylated-Peptide Biopolymer Conjugates. Biomacromolecules 2003;4:1055-67.

[19] West JL, Hubbell JA. Photopolymerized hydrogel materials for drug delivery applications. React Polym 1995;25:139-47.
[20] Hill-West JL, Chowdhury SM, Sawhney AS, Pathak CP, Dunn RC, Hubbell JA. Prevention of postoperative adhesions in the rat by in situ photopolymerization of bioresorbable hydrogel barriers. Obstet Gynecol (N Y) 1994;83:59-64.
[21] Cruise GM, Hegre OD, Scharp DS, Hubbell JA. A sensitivity study of the key parameters in the interfacial photopolymerization of poly(ethylene glycol) diacrylate upon porcine islets. Biotechnol Bioeng 1998;57:655-65.
[22] Bryant SJ, Nuttelman CR, Anseth KS. Cytocompatibility of UV and visible light photoinitiating systems on cultured NIH/3T3 fibroblasts in vitro. J Biomater Sci, Polym Ed 2000;11:439-57.
[23] Stenekes RJH, Hennink WE. Polymerization kinetics of dextran-bound methacrylate in an aqueous two phase system. Polymer 2000;41:5563-9.
[24] Orakdogen N, Okay O. Influence of the initiator system on the spatial inhomogeneity in acrylamide-based hydrogels. J Appl Polym Sci 2007;103:3228-37.
[25] Behravesh E, Jo S, Zygourakis K, Mikos AG. Synthesis of in situ cross-linkable macroporous biodegradable poly(propylene fumarate-co-ethylene glycol) hydrogels. Biomacromolecules 2002;3:374-81.
[26] Hennink WE, Franssen O, van D-W, W. N. E., Talsma H. Dextran hydrogels for the controlled release of proteins. J Controlled Release 1997;48:107-14.
[27] Mawad D, Odell R, Poole-Warren LA. Network structure and macromolecular drug release from poly(vinyl alcohol) hydrogels fabricated via two crosslinking strategies. Int J Pharm 2009;366:31-7.
[28] Peppas NA, Moynihan HJ, Lucht LM. The structure of highly crosslinked poly(2-hydroxyethyl methacrylate) hydrogels. Journal of Biomedical Materials Research 1985;19:397-411.
[29] Flory PJ. Principles of Polymer Chemistry. Ithica, N. Y.: Cornell University Press, 1953.
[30] Lu S, Anseth KS. Release Behavior of High Molecular Weight Solutes from Poly(ethylene glycol)-Based Degradable Networks. Macromolecules 2000;33:2509-15.
[31] Canal T, Peppas NA. Correlation between mesh size and equilibrium degree of swelling of polymeric networks. J Biomed Mater Res 1989;23:1183-93.
[32] Merrill EW, Dennison KA, Sung C. Partitioning and diffusion of solutes in hydrogels of poly(ethylene oxide). Biomaterials 1993;14:1117-26.
[33] Jones M-C, Leroux J-C. Polymeric micelles - a new generation of colloidal drug carriers. Eur J Pharm Biopharm 1999;48:101-11.
[34] Jarrett P, Lalor CB, Chan L, Redmon MP, Hickey AJ. Micelle formation and reaction kinetics of a bioabsorbable polyethylene glycol-oligolactide ABA block copolymer hydrogel. Colloids Surf, B 2000;17:11-21.
[35] Ito K, Tanaka K, Tanaka H, Imai G, Kawaguchi S, Itsuno S. Poly(ethylene oxide) macromonomers. 7. Micellar polymerization in water. Macromolecules 1991;24:2348-54.
[36] Cruise GM, Scharp DS, Hubbell JA. Characterization of permeability and network structure of interfacially photopolymerized poly(ethylene glycol) diacrylate hydrogels. Biomaterials 1998;19:1287-94.
[37] Fiore GL, Klinkenberg JL, Pfister A, Fraser CL. Iron Tris(bipyridine) PEG Hydrogels with Covalent and Metal Coordinate Cross-Links. Biomacromolecules 2009;10:128-33.

[38] Sanabria-DeLong N, Crosby AJ, Tew GN. Photo-Cross-Linked Poly(lactide)-Poly(ethylene oxide)-Poly(lactide) Hydrogels from Self-Assembled Physical Networks: Mechanical Properties and Influence of Assumed Constitutive Relationships. Biomacromolecules 2008;9:2784-91.
[39] Barman SP, Coury AJ, Pathak CP. Biodegradable In-Situ Macromonomers -1: Effect of Hydroxyacids on Micellization. The Fifth World Biomaterials Congress. Toronto, Canada, 1996.
[40] Abd E-R, H. A., El-Arnaouty MB. Properties and biocompatibility of polypropylene graft copolymer films. J Biomed Mater Res, Part B 2004;68B:209-15.
[41] Miller CW, Viswanathan K, Jonsson S, Nason C, Kuang W-F, Yang D, et al. Synergistic effects of N-vinylamides in photopolymerization of simple acrylate formulations. Polym Prepr (Am Chem Soc, Div Polym Chem) 2001;42:811-2.
[42] Jansen JFGA, Houben EEJE, Tummers PHG, Wienke D, Hoffmann J. Real-time infrared determination of photoinitiated copolymerization reactivity ratios: Application of the Hilbert transform and critical evaluation of data analysis techniques. Macromolecules 2004;37:2275-86.
[43] Burdick JA, Lovestead TM, Anseth KS. Kinetic Chain Lengths in Highly Cross-Linked Networks Formed by the Photoinitiated Polymerization of Divinyl Monomers: A Gel Permeation Chromatography Investigation. Biomacromolecules 2003;4:149-56.
[44] Lovestead TM, Burdick JA, Anseth KS, Bowman CN. Understanding multivinyl monomer photopolymerization kinetics through modeling and GPC investigation of degradable networks. Polymer 2005;46:6226-34.

FIGURE 1

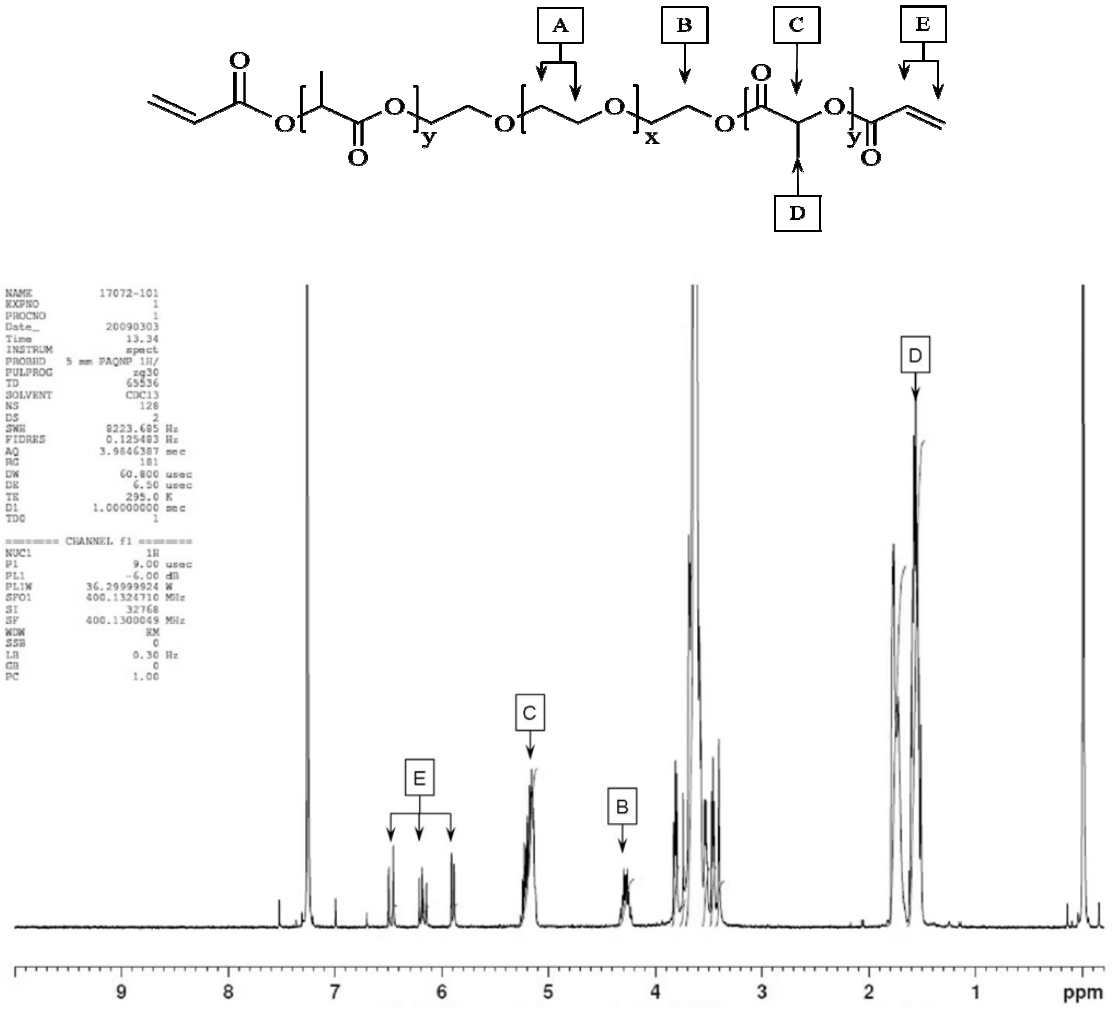
A
B
C
D
E
NAME 17072-101
EXPNO 1
PROCNO 1
Date_ 20090303
Time 13.34
INSTRUM spect
PROBHD 5 mm PAQNP 1H/
PULPROG zg30
TD 65536
SOLVENT CDCl3
NS 128
DS 2
SWH 8223.685 Hz
FIDRES 0.125483 Hz
AQ 3.9846387 sec
RG 181
DW 60.800 usec
DE 6.50 usec
TE 295.0 K
D1 1.00000000 sec
TD0 1
======== CHANNEL f1 ========
NUC1 1H
P1 9.00 usec
PL1 -6.00 dB
PL1W 36.29999924 W
SFO1 400.1324710 MHz
SI 32768
SF 400.1300049 MHz
WDW EM
SSB 0
LB 0.30 Hz
GB 0
PC 1.00
9
8
7
6
5
4
3
2
1
ppm

FIGURE 2

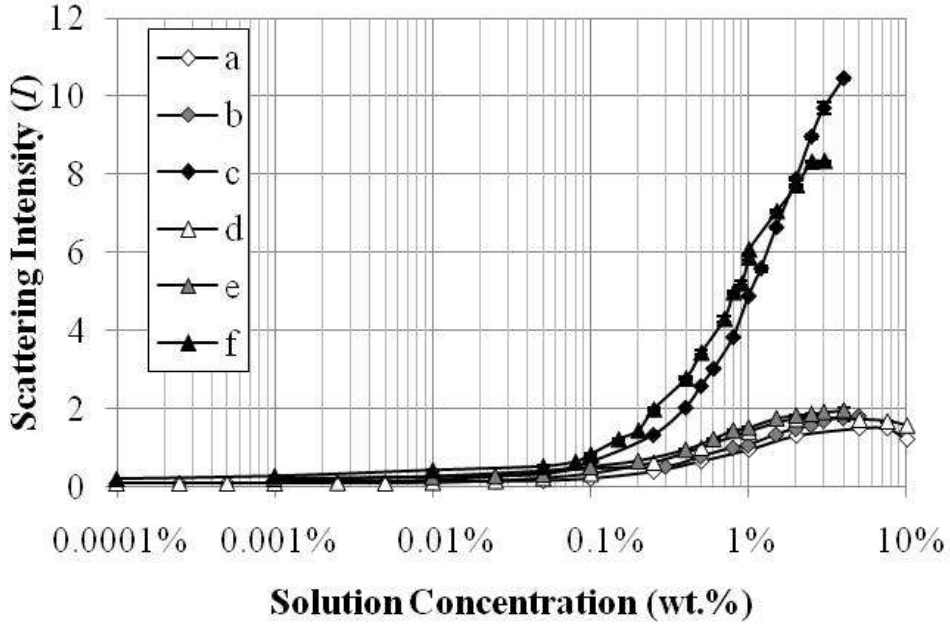
12
10
8
6
4
2
0
Scattering Intensity (I)
a
b
c
d
e
f
0.0001%
0.001%
0.01%
0.1%
1%
10%
Solution Concentration (wt.%)

FIGURE 3

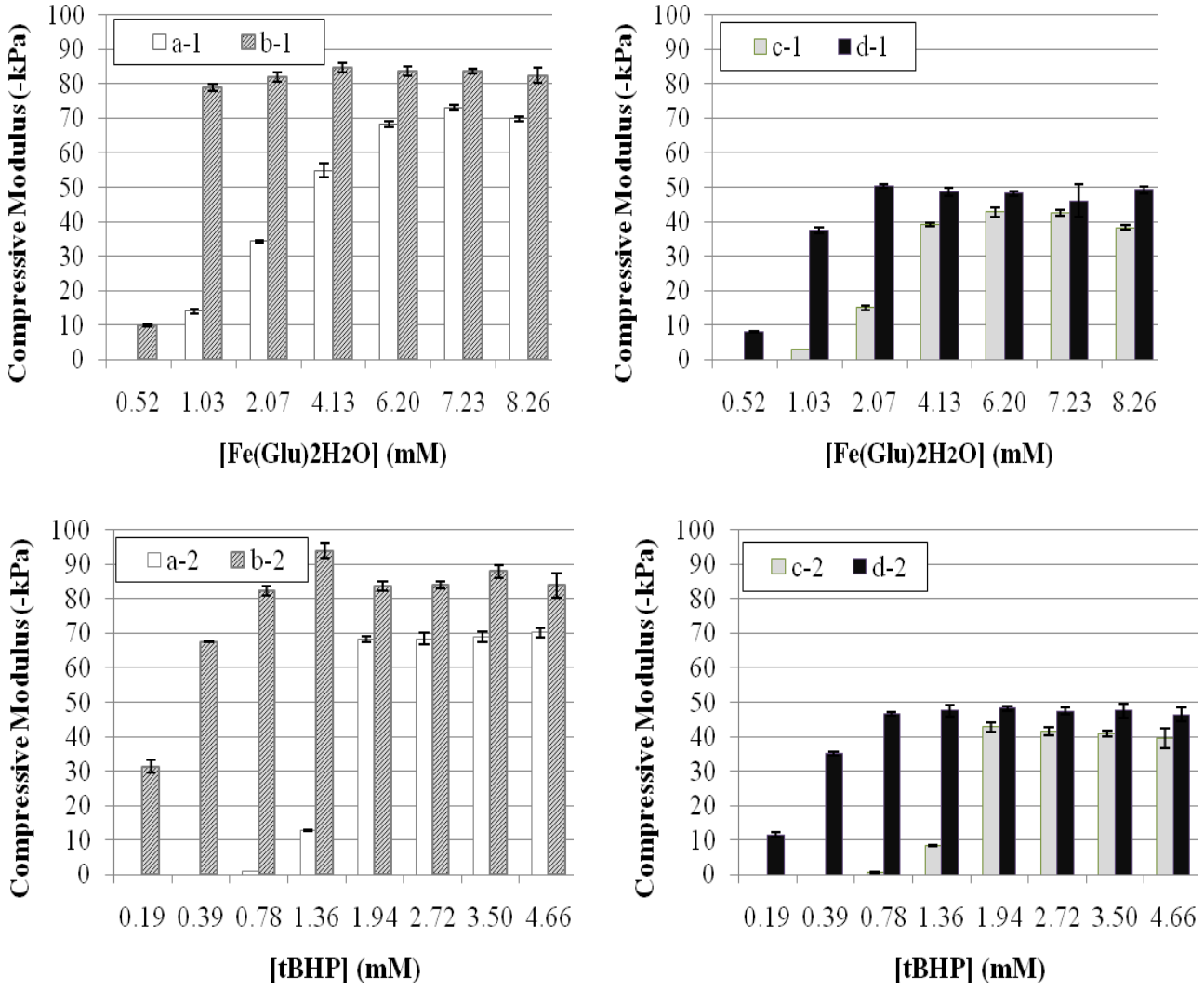
Compressive Modulus (-kPa)
a-1
b-1
0.52 1.03 2.07 4.13 6.20 7.23 8.26
[Fe(Glu)2H2O] (mM)
c-1
d-1
a-2
b-2
0.19 0.39 0.78 1.36 1.94 2.72 3.50 4.66
[tBHP] (mM)

FIGURE 4.

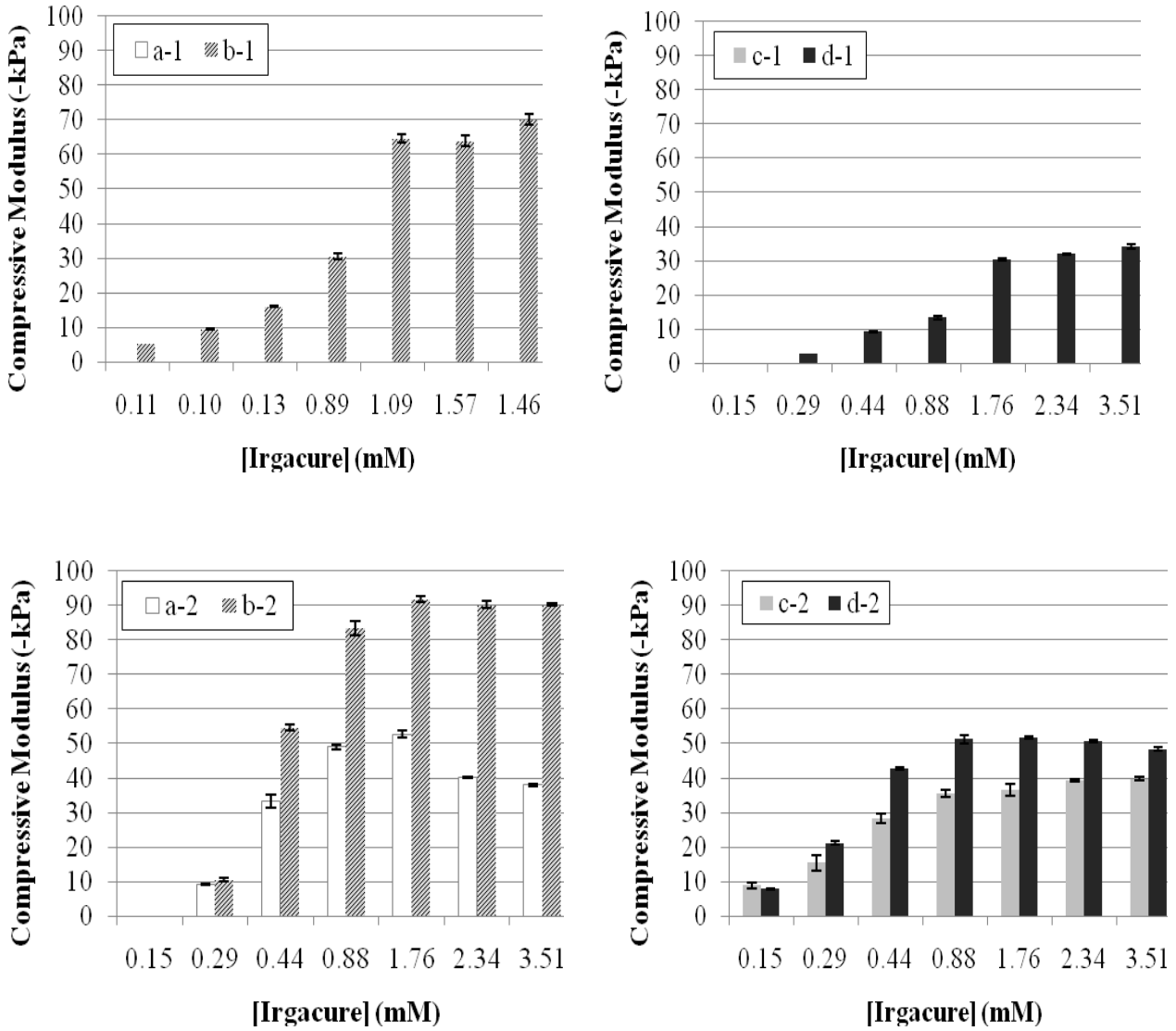
Compressive Modulus (-kPa)
a-1
b-1
0.11 0.10 0.13 0.89 1.09 1.57 1.46
[Irgacure] (mM)
c-1
d-1
0.15 0.29 0.44 0.88 1.76 2.34 3.51
[Irgacure] (mM)
a-2
b-2
0.15 0.29 0.44 0.88 1.76 2.34 3.51
[Irgacure] (mM)
c-2
d-2
0.15 0.29 0.44 0.88 1.76 2.34 3.51
[Irgacure] (mM)

FIGURE 5.

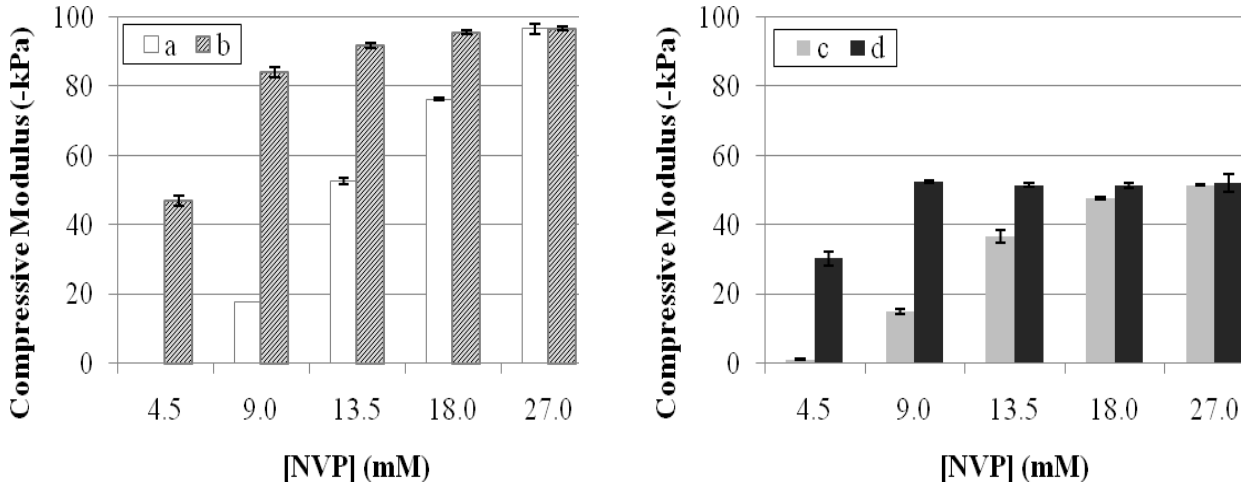
Compressive Modulus (-kPa)
100
80
60
40
20
0
a
b
4.5
9.0
13.5
18.0
27.0
[NVP] (mM)
Compressive Modulus (-kPa)
100
80
60
40
20
0
c
d
4.5
9.0
13.5
18.0
27.0
[NVP] (mM)

EFFECTS OF MOLECULAR WEIGHT DISTRIBUTION ON THE FORMATION OF FIBERS OF ELECTROSPUN POLYSTYRENE

(*Published in the Proceeding of ANTEC™ 2007*)

*Xiaoshu Dai, Satya Shivkumar**

Worcester Polytechnic Institute, Department of Material Science and Engineering, 100 Institute Road, Worcester, MA 01609

Abstract

It is widely recognized that molecular weight distribution (MWD) is an important factor affecting the rheological behavior of polymer solutions. In this contribution, the effects of MWD on the formation of electrospun fibers from polystyrene in THF have been studied. The results are compared with the monodisperse system. The importance of chain entanglements attributed to high molecular weight component within the polydisperse system has been acknowledged. Concentrations for the incipient as well as stable fiber formation in a polydisperse system may be predicted.

Key Words: Molecular weight distribution, electrospinning, polystyrene.

Introduction

Molecular weight distribution (MWD) is an important factor affecting the rheological behavior of a polymer solution. The effects of MWD on polymer blend and melt were studied previously by many groups. Struglinski *el al* [1] analyzed the linear viscoelastic properties of binary polydisperse entangled polymers. They concluded that the behavior of the binary mixture depends both on the relaxation time and weight fraction of the individual component. The zero shear viscosity (η_o) of the mixture is dominated by the weight average molecular weight ($\overline{M_w}$). Powell [2] has introduced an empirical equation for polymer systems which is postulated to be a function of molecular weight distribution. For a bulk polymer, Powell's equation takes the form

of $\eta = \eta_o / [1 + (\tau D)^{2F}]$, in which τ is a representative relaxation time, $F = (\overline{M_n} / \overline{M_w})^x$,. and x is a constant related to molecular shape. For a monodisperse system F=1. Cross [3] indicated while the zero shear viscosity is related to $\overline{M_w}$ or $\overline{M_v}$, the relaxation time is dependent on a higher moment of the distribution curve. Moreover, it was verified previously that the lower shear rate exponent can be obtained from polymer melts and in moderately concentrated solutions for a polydispers system [3]. The value of the exponent must be related to a distribution of relaxation times. In summary, a higher value of distribution gives a lower value of flow parameter but broader shape of the flow curve. Ye *el al* [4] observed a broader relaxation spectrum, a much higher extensional viscosity as well as a slightly smaller zero-shear viscosity (η_o) in a multicomponent system compared to the monodisperse polymer. It was concluded that these differences were attributed to the high molecular weight components in the polydispers system.

Bueche **[**5**]** found that one can describe the viscosity by the relation η= *(const.)* $M_t^{3.5}$, which the molecular weight average appropriate for M_t lies between the weight and *z* average. For molecular weight distributions with M_w/M_n less than about two, M_t is best represented by M_w. Above that value, M_z is a better approximation. However, these latter statements are not precise because M_t appears sensitive to the exact form of the distribution. Reasonable agreement with available experimental data is found. For polydisperse systems, the weight-average molecular weight, M_w, is typically used as the molecular weight.

Electrospinning is an efficient method to produce polymer fibers from solutions. The solution rheology has a significant influence on the electrospun morphologies. In electrospinning, it has been shown that, for a given molecular weight, there is a transition concentration (C_i) at which fibers begin to emerge from the beads and another concentration (C_f) at which a fibrous structure is stabilized [6]. C_i is typically close to the entanglement concentration C_e, at which chain

entanglements in the solution become significant. More recently, Shenoy *el al* [6] defined the entanglement number in solution $(n_e)_{soln}$ according to equation (1):

$$(n_e)_{soln} = \frac{M_w}{(M_e)_{soln}} \qquad (1)$$

in which, M_W is polymer molecular weight, $(M_e)_{soln}$ is solution entanglement molecular weight which can be related to the entanglement molecular weight (M_e) by: $(M_e)_{soln} = M_e/c$, in which c is the solution concentration. Thus, equation (1) can be written as:

$$(n_e)_{soln} = \frac{M_W c}{M_e} \qquad (2)$$

The entanglement molecular weight (M_e) for polystyrene is about 16,600 g/mol [6]. The authors observed the formation of beaded electrospun fibers for values of $(n_e)_{soln}$ equal to 2, and uniform fiber production for $((n_e)_{soln} > 3.5$.

In the polydisperse system, the number of entanglements contributed by each component should be taken into account separately. The total number of entanglements contributed by each component can be calculated based on the weight fraction of each polymer as shown below:

$$n_i = w_i \times M_{w,i} / (M_e)_{soln} \qquad (3)$$

In this contribution, a series of polydisperse polystyrene samples with various concentrations were electrospun from THF solution. The concentrations for the onset of fiber formation as well as the complete fiber formation were determined by SEM analysis. The rheological properties of the aforementioned polystyrene-THF solutions were also studied. The dependence of zero-shear viscosity on the weight average molecular weight as well as the solution concentration was determined. Results are compared with the monodisperse systems. The effects of molecular weight distribution were studied.

Experimental procedure

In order to explore the impact of Molecular weight distribution on the fiber formation during electrospinning, three different MWD numbers between 1.7 and 3.3 were selected. Six nearly monodisperse polystyrene samples with M_W ranging from 19,300 – 1,877,000 g/mol (Scientific Polymer Products, Ontario, NY) were utilized to prepare wide MWD samples with the desired polydispersity. The molecular weight for each component was chosen to cover the range of molecular weight evenly. For each desired MWD, the M_n was kept the same (M_n=400,000g/mol). The weight fraction of each component can be obtained by balancing the weight contributions of each component to the corresponding weight average molecular weight of the desired polydisperse system. The weight fractions necessary to achieve three different MWD numbers, from the 6 monodisperse polymers are summarized in Table 1. It is also possible to examine the fraction of the total number of entanglements by simply using the weight fraction of each component: $n_i=w_iMw/M_e$, which, is also listed in Table 1.

The polydisperse solutions were prepared by dissolving the appropriate amounts of polystyrene in tetrahydrofuran (Sigma-Aldrich). Electrospinning was conducted on these solutions for at least 6 different concentrations. A monodisperse polymer solution was also electrospun. The morphology of the electrospun fibers was examined with a scanning electron microscope (SEM, JSM-840) after sputter-coating the sample with gold-palladium.

The viscosity of the solution at 25°C was measured using a digital rheometer (Brookfield Model DV III). Approximately 0.5 mL of the mixture was placed in the center of the small sample adapter. This sample was sheared for 10 min at 100% Torque to ensure thorough contact between the solution and the cone-plate. The viscosity of the mixture was then measured at desired shear rates. At least 15 different shear rates were used for each measurement. The shear

rate was varied between $0.1s^{-1}$ and $450s^{-1}$. The zero-shear viscosity (η_o) was calculated based on power law equation:

$$\eta=\eta_o\gamma^n \qquad (4)$$

in which γ is the strain rate and n is the flow index.

Results and Discussion

The weight fraction of each component can be obtained by equating the sum of contributions of a certain number of each component to the desired number average molecular weight (M_n) of the polydisperse mixture. While a concept of entanglement number is introduced to examine the fraction of total number of entanglements contributed by each, it is clear that the contribution of higher molecular weight components to the entanglement number is much higher than the low molecular weight components.

For different MWD samples, the concentrations for the onset of fiber formation and complete fiber formation can be predicted by rearranging equation (2). Moreover, calculation can only be made by assuming these polydisperse systems as monodisperse samples with the corresponding weight average molecular weight, the critical concentrations can then be calculated by setting n_e=2 and 3.5 for onset of fiber formation and complete fiber formation, respectively. The results are listed in Table 2.

Jamieson *el al* [7] reported the zero-shear viscosity of semi dilute solutions of monodisperse polystyrene with different molecular weights in THF. The zero-shear viscosity data for M_W=390,000g/mol and M_W=600,000g/mol were read off and replotted as the solid line shown in Figure 2 (c) and (d). Two regions are observed indicating the different entanglement status in the solution. With a slope of 1.5, region I corresponds to the dilute region where few entanglements may be present among the macromolecules in the solution. Region II represents

the entangled region with a slope of 3.4. The dependence of the zero-shear viscosity on the solution concentration shifted dramatically with increasing solution concentrations. A slope on the order of 3.4 (region II) can be obtained for all molecular weights which were also previously reported for the monodisperse system [7]. The corresponding concentration of the intersection of the curves is defined as the onset of entanglements. A critical zero-shear viscosity with a value in the order of 0.01 Pa·s was reported by Jamieson *el al* [7] for a series of monodisperse polystyrene samples dissolved in THF. The molecular weights of these samples covered from 390,000g/mol to 7,800,000g/mol. It was reported the critical transition zero-shear viscosity is independent of molecular weight.

The molecular weight (M_W) in the present study for MWD=1 and 1.7 correspond to 393,400g/mol and 590,000 g/mol, the zero-shear viscosity data are plotted in the same graph (Figure 2 curves (a) and (b)). It can be observed that, for MWD=1, the zero-shear viscosities are almost identical to what was reported in the literature for the monodisperse sample. Furthermore, the data exhibit the same slopes of 1.7 and 3.4 for the dilute region and entangled region, respectively. The zero-shear viscosity data of the polydisperse sample with MWD=1.7 are shown as curve b in Figure 2. Having a molecular weight of 590,000g/mol, the zero-shear viscosity follows the same trend as the monodisperse sample with a slope of 1.5 for the dilute region and a slope of 3.4 for the entangled region. In this case, however, the intersection appears at a lower concentration.

The zero-shear viscosity data as a function of solution concentration for all the samples examined in this study are plotted in Figure 3. The power law equations for the two regions shown in Figure 3 are summarized in Table 3. It can be observed that the intersections for higher MWD samples shifted to the lower values of zero-shear viscosity. With the broadening of

molecular weight distribution, the fraction of high molecular molecules increased. By occupying larger hydrodynamic volumes, the presence of the high molecular weight fractions leads to the early onset of entanglement at low concentrations. On the other hand, increasing the low molecular weight fractions may result in lowering of the zero shear viscosity in response to the shear force at these concentrations. The concentrations at the intersections for different MWD samples can be calculated based on the equations displayed in Table 3. In this case, the onset of entanglement concentration can be related to the corresponding molecular weight of the mixture according to the following power law relation ($R^2 = 0.991$):

$$c_e = 17903(M_W)^{-0.8087} \qquad (5)$$

Electrospinning was conducted with these solutions. The SEM photographs in Figure 4 show the structure obtained at various concentrations for samples with MWD=1.7. When a concentration of c=0.01g/mL was used, only beads can be observed in the electrospun structure due to the insufficient viscoelastic property of the solution. Fibers started to appear at a concentration of c=0.024g/mL as shown in Figure 5 (b). Thus, this concentration is determined necessary for the onset of entanglements. Beaded fibers were obtained above this concentration while complete fibrous structures were obtained at c=0.12g/mL, as shown in Figures 5(c) and (d). The transition concentrations for all the samples can then be determined.

The transition concentrations are summarized in Fig. 5 for various molecular weights. The transition concentrations for monodisperse systems which were reported in the literature as well as those calculated by the entanglement number model are also shown for comparison. As the MWD increases, the concentration for the onset of entanglements decreases dramatically. The onset of entanglement concentrations obtained by SEM analysis have slightly lower values compared to the results obtained from viscosity measurements. These differences may be due to

the rapid evaporation of the solvent during electrospinning which may lead to a slight increase in the effective solution concentration. The onset of entanglement concentrations have much lower values for the polydisperse sample compared to the monodisperse samples (shown as curve (d) in Figure 5). The transition concentrations calculated from equation (2) by fixing the entanglement number to 2 and 3.5 concentration are also plotted as curves (e) and (f). A much broader transition region can be observed with increasing molecular weight distribution. The presence of fibers at very low concentration indicates the early emergence of entanglements between molecules within the solution. The high molecular weight fractions dominate the entanglement status of the solution, while the effect of low molecular weight fragments may be ignored at these concentrations.

Conclusions

The effects of molecular weight distribution on the formation of electrospun fibers from polystyrene in THF have been studied. A fibrous structure can be obtained at a lower concentration in polydisperse samples than in a monodisperse polymer. The higher molecular weight fragments may contribute to entanglements even at low concentrations and thereby stabilize a fibrous structure.

References

1. M.J. Struglinski, and W.W. Graessley, "Effects of polydispersity on the linear viscoelastic properties of entangled polymers. 1. Experimental observations for binary mixtures of linear polybutadiene", *Macromoecules,* 18, 2630 (1985).
2. A. Powell, "The fractionation of polypropylene oxide polymerized by ferric chloride", *Polymer*, 8, 211(1967).
3. M. Cross, "Polymer rheology: Influence of molecular weight and polydispersity", *J.Appl. Polymer Sci.*, 13, 765 (1969).
4. X. Ye, and T. Sridhar, "Effects of the Polydispersity on Rheological Properties of Entangled Polystyrene Solutions", *Macromolecules,* 38, 3442 (2005).
5. F. Bueche, "Diffusion of Polystyrene in Polystyrene: Effect of Matrix Molecular Weight", *J. Chem. Phys.,* 48, 1410 (1968).

6. S.L. Shenoy, W.D Bates. H.L. Frisch, and G.E. Wnek, "Role of chain entanglements on fiber formation during electrospinning of polymer solutions: good solvent, non-specific polymer–polymer interaction limit",*Polymer,* 46, 3372 (2005).
7. A.M. Jamieson, and D. Telford, "Newtonian viscosity of semidilute solutions of polystyrene in tetrahydrofuran", *Macromolecules,* 15, 1329 (1982).

Table 5 Mass fractions (w_i) of the monodisperse samples used to prepare a polydisperse polymer of the desired Molecular Weight Distribution (MWD). The molecular weight ($M_{w,i}$) of the monodisperse and the polydispersity in these samples are also shown. The entanglement number ($w_i*M_{w,i}/M_e$) calculated from equation (2) is also shown for each PDI.

$M_{w,i}$ (g/mol)	Polydispersity	PDI=1.7		PDI=2.5		PDI=3.3	
		w_i	$w_i*M_{w,i}/M_e$	w_i	$w_i*M_{w,i}/M_e$	w_i	$w_i*M_{w,i}/M_e$
19,300	1.0663	0.0034	0.0040	0.0053	0.0061	0.0075	0.0087
44,100	1.0704	0.0078	0.0208	0.0144	0.0383	0.0256	0.0681
97,400	1.0041	0.0173	0.1013	0.0531	0.3116	0.0754	0.4427
393,400	1.1588	0.6974	16.5274	0.4290	10.1676	0.1524	3.6107
1,045,000	1.0740	0.2408	15.1604	0.2935	18.4739	0.4047	25.4775
1,877,000	1.1348	0.0333	3.7624	0.2047	23.1461	0.3344	37.8103

Table 6 Concentrations calculated for the entanglement number model by rearranging equation (2).

MWD	Corresponding M_W (g/mol)	n_e=2	n_e=3.5
1	393,400	0.0844	0.1477
1.7	590,566	0.0562	0.0984
2.5	865,586	0.0384	0.0671
3.3	1,119,137	0.0297	0.0519

Table 7 Power law equations for the curves shown in Figure 3.

MWD	Region I	Region II
1	$Y = 6368.5\ x^{1.7881}$	$y = 725074x^{3.478}$
1.7	$Y = 3648.7x^{1.5423}$	$y = 2000000x^{3.452}$
2.5	$Y = 4376.6x^{1.4398}$	$y = 3000000x^{3.0188}$
3.3		$y = 4000000x^{2.8701}$

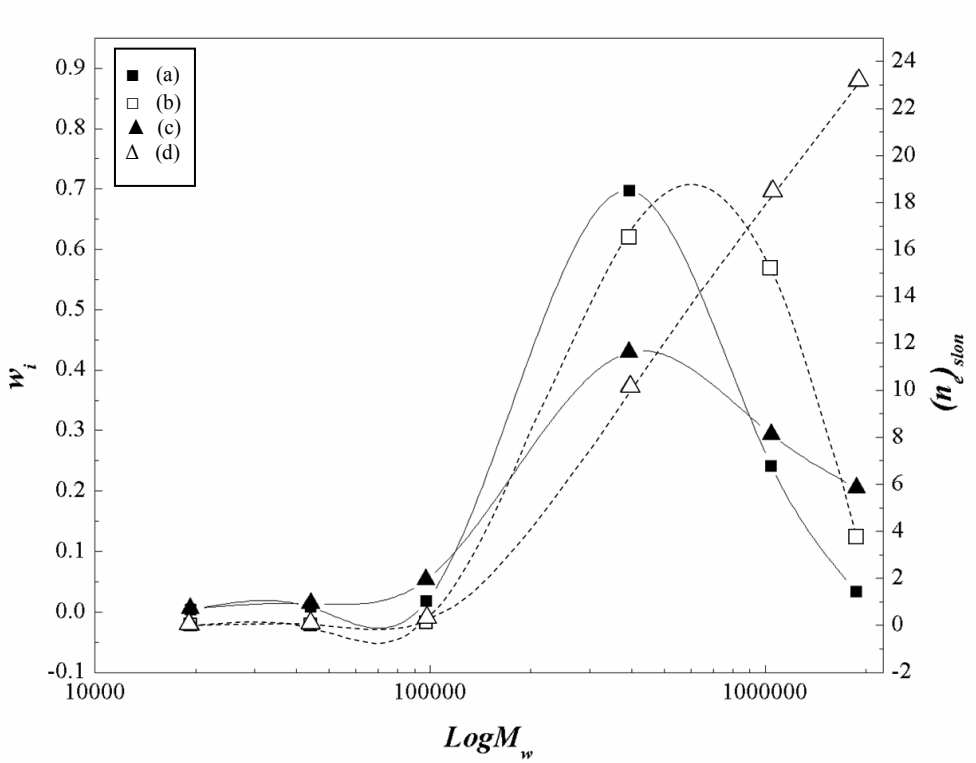

Figure 1 Molecular distribution for (a) MWD=1.7, and (c) MWD=2.5. The contribution of the entanglement number for each molecular fragment is also shown (b) MWD=1.7, and (d) MWD=2.5.

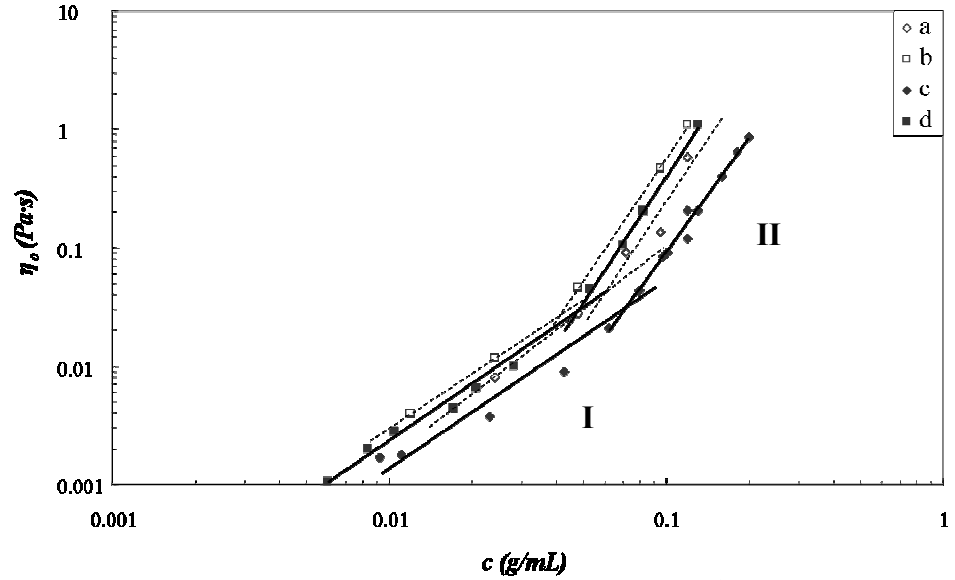

Figure 2 Zero shear viscosities (η_o) of polystyrene in THF at 25°C obtained in this study: (a) M_n=393,400g/mol, MWD=1, and (b) M_n=393,400g/mol MWD=1.7. (c) Polystyrene (M_W=390,000g/mol, MWD=1), (d) Polystyrene (M_W=600,000g/mol, MWD=1) in THF at 30°C obtained by Jamieson *el al* [7]. The trendlines have the slope of 3.4 and 1.7 for region I and II, respectively.

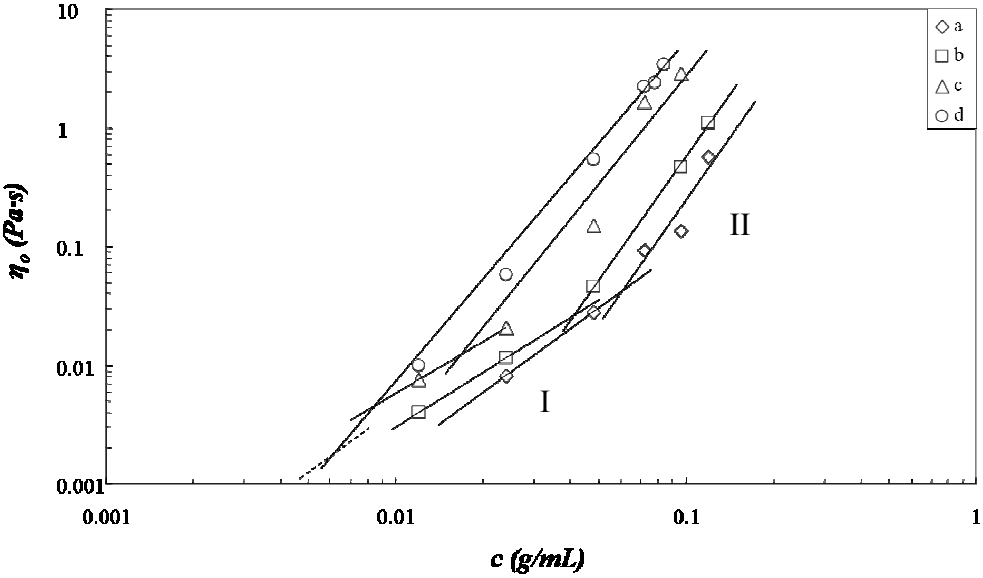

Figure 3 Zero-shear Viscosity as a function of solution concentration for polystyrene/THF solutions. (a) MWD=1, (b) MWD=1.7, (c) MWD=2.5, and (d) MWD=3.3.

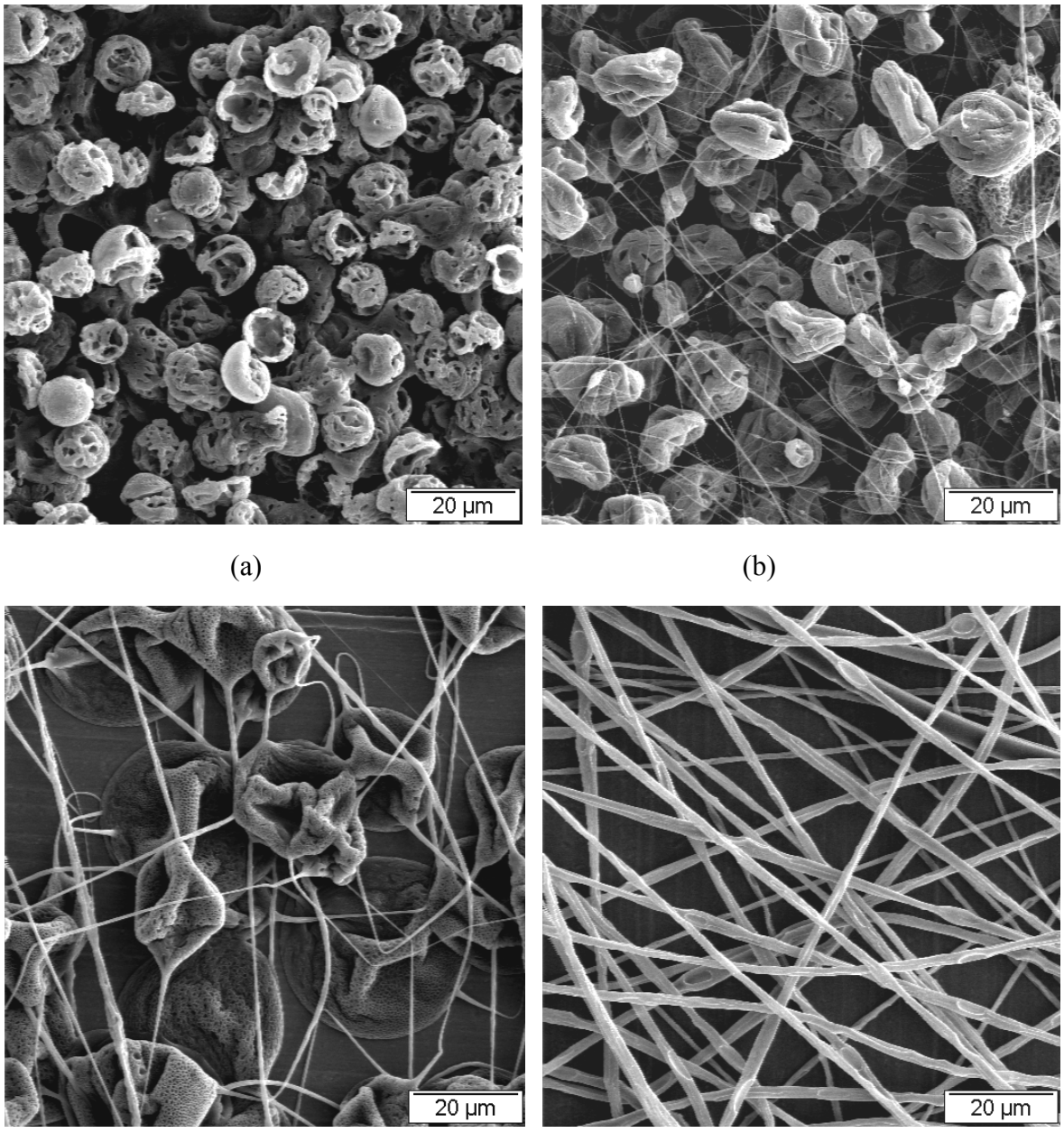

Figure 4 SEM photographs showing (a) complete bead structure (MWD=1.7 *c*=0.01g/mL), (b) onset of fiber formation (MWD=1.7 *c*=0.024g/mL), (c) beaded fibers (MWD=1.7 *c*=0.097g/mL), and (d) complete fibrous structure (MWD=1.7 *c*=0.12 g/mL).

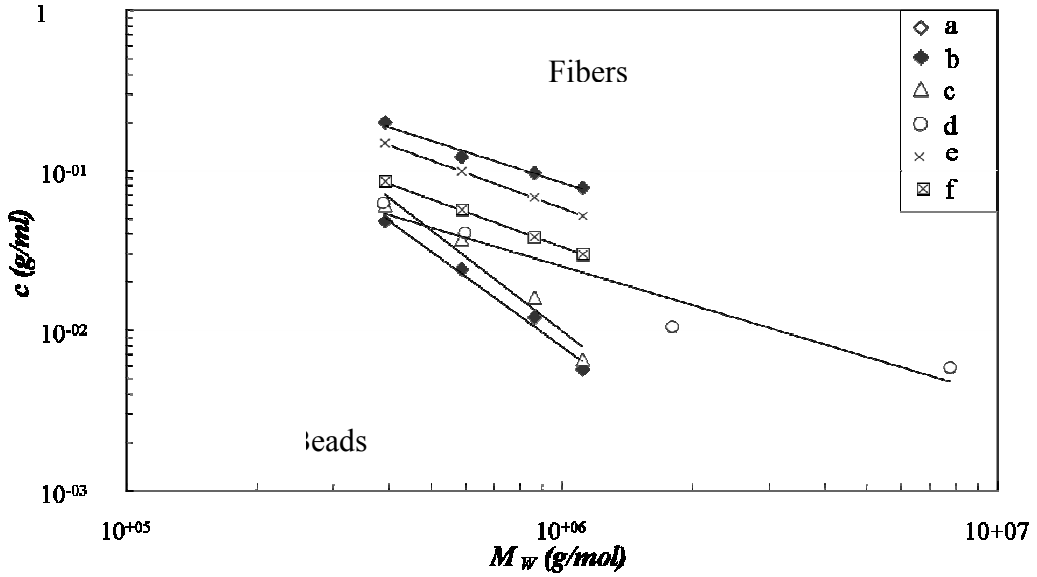

Figure 5 Concentrations for (a) complete fiber formation, and (b) onset of fiber formation obtained from SEM analysis of the electrospun samples as a function of molecular weight. The concentration for the onset of entanglements calculated from zero-shear viscosity measurements from this study (c), and the data of Jamieson *el al* [7] (d) for monodisperse systems are also shown for comparison. The limiting values for the onset of fibers, n_e=2, (e) and complete fiber formation, n_e=3.5, (f) based on the model of Shenoy *et al* [6] are plotted.

MOLECULAR INTERACTIONS BETWEEN POLYVINYLPYRROLIDONE AND SURFACTANT: THE EFFECTS OF COIL DIMENSIONS ON ELECTROSPUN MORPHOLOGIES

(Submitted to the *Journal of Applied Polymer Science*)

Xiaoshu Dai, and Satya Shivkumar*

Department of Materials Science and Engineering, Worcester Polytechnic Institute,

100 Institute Rd., Worcester, MA 01609, USA

Abstract

The effects of molecular interactions between polyvinylpyrrolidone (PVP) and sodium dodecyl sulfate (SDS) on polymer coil dimension in their aqueous precursors and the electrospun morphology were investigated over a broad range of concentrations of the surfactant, from 0.1 mM to 200 mM, and as a function of three molecular weight grades of PVP. Zero-shear viscosity (η_0) measurements were used to characterize the chain dimension. Results suggest that SDS may bind to the polymer chain and affect the PVP coil size through intramolecular interactions. Two stages of binding were observed and separated by a surfactant minimum effective concentration (c_m) regardless of the polymer molecular grades and concentration. At $c < c_m$, surfactant anions can bind to the polymer molecule leading to the contraction of the polymer coil while at $c \geq c_m$, surfactant micelles may bind to the polymer molecule resulting in the expansion of the coil. These solutions were electrospun and the morphologies were studied by scanning electron microscope (SEM). Pure PVP aqueous solutions deposited as beads or beaded fibrous structures and can be stabilized by the addition of the surfactant. Experimental results demonstrated that in moderately entangled solutions, above c_m, surfactant affected polymer solutions to yield fine uniform fibers. In the polymer solution with no entanglements, a decrease in uniformity was observed in the electrospun pattern with the addition of surfactant. A model was established to better describe the experimental observations.

Introduction

The interactions between surfactant and suitable polymers have attracted greater attention in the production of nanofibers by electrospinning.[1] A number of nonionic polymers have been

electrospun with ionic surfactants as a co-spinning agent to form uniform fibrous structures.[2-7] The complexation between polymer and surfactant is best known to lead to a low surface tension[8] and high solution conductivity [8.9] which favor the stability of the solution jet and the formation of uniform fibrous structures.[10] In a polymer/solvent/surfactant system, it was observed that the anionic surfactant can bind cooperatively to the nonionic polymer.[11] It is well established that the interaction of a nonionic polymer with an anionic surfactant can result in polyelectrolyte properties to the nonionic polymer.[12-14] Beyond the surfactant critical micelle concentration (CMC), the polymer surfactant complex is viewed as composed of a series of spherical micelles with their surfaces covered by polymer segments and connected by strands of the same polymer molecules, thus resembling a "necklace of beads", the so-called 'necklace model'.[15] However, below this concentration, polymer coil contraction was observed depending on polymer chain length. It was reported that contraction of the hydrodynamic volume occurred rather than expansion due to charge repulsion depending on the anion concentration and polymer chain length.[16]

Researchers have been focusing on the effects of the addition of surfactant on polymer electrospinnability with surfactant concentration well above the surfactant CMC. Systematic studies on the effects of the addition of surfactant on electrospun polymer fibrous structures are not readily available. In this contribution, polyvinylpyrrolidone (PVP) and sodium dodecyl sulfate (SDS) were selected to study the effects of molecular interactions between polymer and the anionic surfactant on the electrospun morphology of their aqueous precursors. The PVP-SDS aqueous system is one of the most investigated model systems.[16,17] Experiments were conducted

over a broad range of the surfactant concentration, from 0.1 mM to 200 mM. The effects of molecular weight on the structure were also studied.

Materials

PVP is characterized by the K-value, or the Fikentscher's viscosity coefficient, which is used mostly for polyvinylpyrrolidone and vinylpyrrolidone copolymers.[18] The K-value is based on kinematic viscosity measurements, given by the Fikentscher equation[19]:

$$\frac{\log(\eta_{rel})}{c} = \frac{75K_0^2}{1+1.5K_0c} + K_0 \quad (1)$$

where c represents the concentration in g/100mL; η_{rel} represents the relative viscosity as compared to the solvent; and K_0 represents K/1000. The K-value can be directly calculated by rearranging the Fikentscher equation:

$$K = \frac{\sqrt{300c\log(\eta_{rel}) + (c+1.5c\log(\eta_{rel}))^2} + 1.5c\log(\eta_{rel}) - c}{0.15c + 0.003c^2} \quad (2)$$

Linear poly(vinylpyrrolidone)(PVP) with different molecular weights and grades, labeled as average molecular weight M_w=1,300,000g/mol with K-value=90~100 (PVP1300), M_w=36,000g/mol with K-value=80~100 (PVP360), and M_w=55,000g/mol with the K-value =8~34 (PVP55) and sodium dodecyl sulfate (SDS) were purchased from Sigm-Aldrich (St. Louis, MO). Deionized (DI) water was used for preparing all solutions.

PVP aqueous solutions were prepared by dissolution in DI water at ambient temperature (21.0 ^{o}C) to achieve the desired concentration. Concentrated SDS aqueous solutions were prepared separately and added into the PVP solution providing the desired molar concentrations ranging from 0.1 mM to 200 mM. Homogeneous solutions were obtained after mixing.

The viscosity of the solutions at ambient temperature (21°C) was measured using a digital cone-plate rheometer (Brookfield Model DV III, Middleboro, MA) equipped with a cone-spindle (CPE-40). Approximately 0.5 mL of the mixture was placed in the center of the small sample adapter. This sample was sheared for 2 min at 100% Torque to ensure thorough contact between the solution and the cone-plate. The viscosity of the mixture was then measured at desired shear rates varied between $0.1s^{-1}$ and $250s^{-1}$. The zero-shear viscosity (η_o) is calculated based on power law equation:

$$\eta=\eta_o \dot{\gamma}^{n-1} \qquad (3)$$

in which $\dot{\gamma}$ is the strain rate and n is the flow index.

The solution mixture was loaded in a 1mL syringe equipped with an 18 gauge needle (inner diameter = 0.84 mm, 51 mm long). The syringe was mounted horizontally on a syringe pump (EW-74900-00, Cole-Parmer). A grounded aluminum foil collector (10 cm × 10 cm) was positioned 10 cm from the tip of the needle. The syringe pump was calibrated to achieve a flow rate of 0.1 mL/h for all experiments. A potential of 20 kV was applied to the needle immediately after a pendant drop formed at the tip. The electrospun samples were sputter coated with gold-palladium and examined in a JEOL JSM-7000F (Tokyo, Japan) scanning electron microscope (SEM).

Results and discussion

The zero-shear viscosity (η_0) of PVP aqueous solutions as a function of concentration are shown in Figure 1. Within the concentration range, PVP360 solutions show identical viscosity behavior to PVP1300. This is expected since similar *K*-values were provided by the supplier. A broader molecular weight distribution in PVP360 polymer was anticipated in this case. Identical

viscosity behavior indicates the potentially identical intrinsic viscosity. With increasing of the solution viscosity, a sharp increase of zero-shear viscosity was observed, with a dependence on solution concentration from the first power to approximately the fourth power. A concentration of 7%(w/v) for PVP1300 and PVP360 corresponds to the transition concentration from dilute to semi-dilution regime (c^*) or the on-set of entanglement. A similar trend was observed in the aqueous solutions of PVP55 with a delayed transition concentration, a value of 35%(w/v), as shown in Figure 1 (c). To prepare the electrospinning precursor, a concentration of 15%(w/v) PVP1300 was selected to achieve a $c>>c^*$, 10%(w/v) was selected for both PVP1300 and PVP360 to achieve a $c>c^*$ while a solution concentration of 30%(w/v) was chosen for PVP55 to achieve $c<c^*$. The 10%(w/v) solution of PVP with *K*-value=80-100 has a viscosity of 400 mPa·s while a 30%(w/v) of PVP with *K*-value=28-34 gives a viscosity of 90 mPa·s in agreement with values supported in the literature.[20]

The electrospun morphologies of the polymer solutions are shown in Figure 2. The 15%(w/v) solution of PVP130 achieved a complete fibrous structure with average fiber diameter of 238±8nm. However, 10%(w/v) solution of PVP1300 and PVP360 deposited as beaded fibrous structure, while 30%(w/v) of PVP55 yielded a complete beaded structure. The poor electrospinnability of the lower concentration and lower M_w solutions indicated insufficient entanglements between polymer molecules and/or weak interactions between polymer and solvent molecules in solution. Varying amounts of SDS were then added to these PVP solutions in order to determine the minimum effective surfactant concentration (c_m) at which a uniform fibrous structure can be produced.

The viscosities of PVP solutions with various SDS concentrations were first measured. Results are plotted in Figure 3. At a low SDS concentration, the solution viscosities continuously decrease with increasing SDS concentration. The decreasing of solution viscosity at low SDS concentration can be explained as follows. In an aqueous solution of PVP and SDS, at concentrations lower than the critical micelle concentration (CMC) of SDS (8.2 mM[21]), it is the SDS anions binding with PVP molecules. By absorbing the anions, PVP essentially becomes a charged polyelectrolyte, the charges stretching the polymer chain just as they do in structural polyelectrolytes. It was reported that the anions have a salting-in effect on the amide groups (=N-CO) but a salting out effect on the hydrocarbon backbone of the PVP chain.[17] As a result, the anions will attract the amide groups while repel the rest. The electrostatic repulsion may lead to the rearrangement of the coil structure of the PVP into a smaller dimension. Thus the anion bounded molecules tend to be salted-out from the solvent. With increasing concentration of SDS, the charge density of PVP chain is anticipated to increase. The increasing repulsion between the charges may further disturb the formation of inter-molecular bonds between PVP coils. Overall, the intra-molecular interactions between the surfactant anions bind to the polymer segments and lead to the shrinking of the polymer coil. This shrinking effect induces a decrease in precursor viscosity. The viscosity attained a minimum value at approximately 2-5 mM of SDS for PVP1300 and PVP360 solutions (Figure 3 (a), (b) and (c)). The minimum viscosity value occurs at 10-20 mM for PVP55 indicating the shrinking effects of SDS binding to shorter PVP chain act over a broad concentration range.

The electrospun morphologies of 15%(w/v)PVP1300 and 10%(w/v) PVP1300 and PVP360 solution containing 5 mM SDS are shown in Figures 4 (a-1), (b-1) and (c-1). Compared to

Figure 2 (a), (b) and (c), with polymer molecules having a smaller coil dimension, there are no significant structural differences observed. In electrospinning, it is postulated that a decreasing of surface tension and an increasing of solution conductivity are associated with non-ionic polymer binding with ionic surfactant.[10] Thus, these effects counter balance with the shrinking effect which in turn yields identical structures to the surfactant-free polymer solutions.

The viscosity starts to increase at about 10-20 mM of [SDS] after attaining a minimum. This is followed by dramatic rise in viscosity with further increase in SDS concentration. The on-set of the transition concentration, which can also be recognized as the minimum effective surfactant concentration (c_m) is marked as 20 mM as shown in Figure 3. It should be noticed that this value is much higher than the surfactant CMC and is independent of polymer molecular grades and concentration. The electrospun structures of the PVP1300 and PVP360 solutions with 20 mM SDS are shown in Figure 4(a-2), (b-2) and (c-2). Identical electrospun structure was observed for 15%(w/v) PVP1300 solution with a slightly larger fiber size (289±13nm). In the electrospun pattern of 10%(w/v) PVP1300 and PVP360 solutions, bead-free fibrous structures with uniform size distributions were obtained. The average fiber diameter was approximately 103 ±13nm. For the precursors of polymers with some degree of entanglements (e.g. 10%(w/v) PVP1300 and PVP360), at $c_{[SDS]}=c_m$, surfactant micelles start to bind to the polymer segments. The excluded volume effect led to chain expansion into larger hydrodynamic volumes. More entanglements between coils maybe obtained. The increase of zero-shear viscosity is the direct response to the excluded volume effect. Moreover, Klech *et al* [16] reported the decreased values of the Higgins constant with increasing of SDS concentration (within the range of 20 to 70 mM) which provide more favorable interactions between polymer and solvent molecules. With more and more

micelles binding to the polymer, as a result of further expansion of the coil dimension, the electrospun fiber diameter keeps increasing as shown in Figure 4 (a-3) (b-3) and (c-3).

The addition of surfactant has identical effects on the viscosity behavior over the same SDS concentration range on the 30%(w/v) PVP55 solution, as shown in Figure 3(d). However, introducing large amount of the anions into the polymer solution with no entanglements may result in a great gain in entropy, which can be a major driving force for instability of the solution jet during electrospinning process. The electrospun structures of 30%(w/v) PVP55 with 5 mM, and 20 mM SDS are shown in Figure 4 (d-1), and (d-2), respectively. The beaded structure with broad bead-size distribution and the presence of large amount of smaller beads with diameters less than 40 nm can be an indication of random break down of the solution jet and inconsistent polymer flow. No fibrous structures were obtained. The binding of surfactant micelles with polymer chain at $c_{[SDS]} >> c_m$ led to a slight increase in solution viscosity. This increase in viscosity was more likely due to the inhomogeneous locally entangled PVP chain at very high SDS concentration, which may lead to the formation rod-like structures at very high surfactant concentration, as shown in Figure 4(d-3). However, beaded structures remained due to the limited overall entanglements in the precursor.

A schematic illustration of binding sequence between PVP and SDS in an aqueous solution while keeping the polymer concentration constant with increasing surfactant concentration is shown in Figure 5. A PVP coil in its aqueous solution is shown on the left which is followed by the coil structures of the two stages binding with the surfactant. When $c_{[SDS]} < c_m$, surfactant anions bind to the PVP molecules, the coil size decreases due to the shrinking effect from the intramolecular

interactions. This corresponds to the decrease in viscosity. However, the electrospun structures remain unchanged due to the increase in surface tension and solution conductivity which counter balance the shrinking effect. At $c_{[SDS]} \geq c_m$, surfactant micelles bind to the PVP molecules. The excluded volume effect leads to the molecule coils to expand which results in the increase in viscosity and sufficient entanglements. Uniform fibrous structure with nano-sized fibers can be obtained under these conditions.

Conclusions

Measurements of solution viscosity revealed that surfactants are able to modulate polymer coil dimension via intramolecular interactions. A minimum effective surfactant concentration c_m =20 mM was observed for all PVP/SDS aqueous solutions regardless the PVP molecular grades and solution concentration. This concentration is highly desirable for polymer solutions with some degree of entanglements to yield uniform fine fibrous structure. However, for polymer solutions with no entanglements, the addition of the micelles may not be beneficial.

Reference

1. Zeng, J.; Xu, X.; Chen, X.; Liang, Q.; Bian, X.; Yang, L.; Jing, X. J Controlled Release 2003, 92, 227.
2. Bhattarai, N.; Edmondson, D.; Veiseh, O.; Matsen, F. A.; Zhang, M. Biomaterials 2005, 26, 6176.
3. Wang S.-Q.; He, J.-H.; Xu, L. Polym Int 2008, 57, 1079.
4. Nagarajan, R.; Drew, C.; Mello, C. M. J Phys Chem C 2007, 111, 16105.
5. Dror, Y.; Salalha, W.; Khalfin, R. L.; Cohen, Y.; Yarin, A. L.; Zussman, E. Langmuir 2003, 19, 7012.
6. Zhao, Y.; Wang, H.; Lu, X.; Li, X.; Yang, Y.; Wang, C. Mater Lett 2008, 62, 143.
7. Lin, T.; Wang, H.; Wang, H.; Wang, X. Nanotechnology 2004,15, 1375.
8. Yao, L.; Haas, T. W.; Guiseppi-Elie, A.; Bowlin, G. L.; Simpson, D. G.; Wnek, G. E. Chem Mater 2003, 15, 1860.
9. Pérez-Rodríguez, M.; Varela, L. M.; García, M.; Mosquera, V.; Sarmiento, F. J Chem Eng Data 1999, 44, 944.
10. Kriegel, C.; Kit, K. M.; McClements, D. J.; Weiss, J. *Food Biophys.*, 2009, 4, 213.

11. Prasad, M.; Palepu, R.; Moulik, S. P. Colloid Polym Sci 2006, 284, 871.
12. Jones, M. N. J Colloid Interface Sci 1967, 23, 36.
13. Francois, J.; Dayantis, J.; Sabbadin, J. Eru Polym J 1985, 21, 165.
14. Brackman, J. C. Langmuir 1991, 7, 469.
15. Sen, S.; Sukul, D.; Dutta, P.; Bhattacharyya, K. J Phys Chem A, 2001, 105, 7495.
16. Klech, C. M.; Cato III, A. E.; Suttle III, A. B. Colloid Polym Sci 1991, 269, 643.
17. Eliassaf, J.; Eriksson, F.; Eirich, F. R. J Polym Sci 1960, 47, 193.
18. Kroschwitz, J. I., Ed. Encyclopedia of Polymer Science and Engineering; Wiley: New York, 1989, Vol. 17.
19. Kline, G. M. Modern Plastics 1945, Nov., 157.
20. Dornelas, C. B.; Resende, D. K.; Tavares, M. I. B.; Gomes, A. S.; Cabral, L. M. Polímeros 2008,18, 187.
21. Shirahama, K.; Kashiwabara, T. J Colloid Interface Sci 1971, 36, 65.

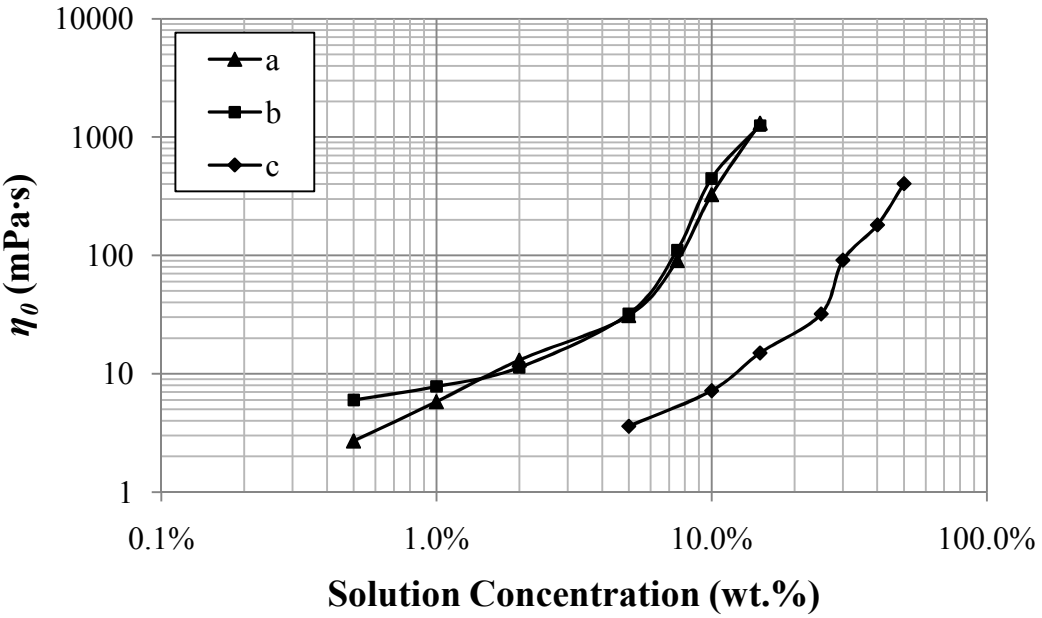

Figure 5 Zero-shear viscosity (η_0) as a function of PVP solution concentrations for different PVP molecular grades, (a) 1,300,000g/mol *K*-value=90-100, (b) 360,000g/mol *K*-value=80-100, and (c) 55,000g/mol *K*-value=28-34.

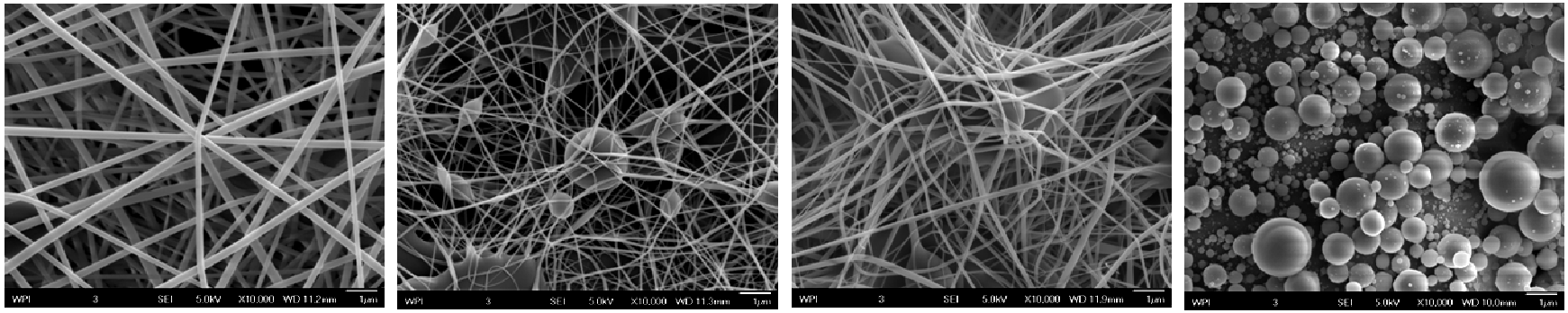

(a) (b) (c) (d)

Figure 6 SEM micrographs showing the electrospun structures from PVP aqueous solutions, (a) 15%(w/v)PVP1300, (b)10%(w/v) PVP1300, (c) 10%(w/v) PVP360, and (d) 30%(w/v) PVP55.

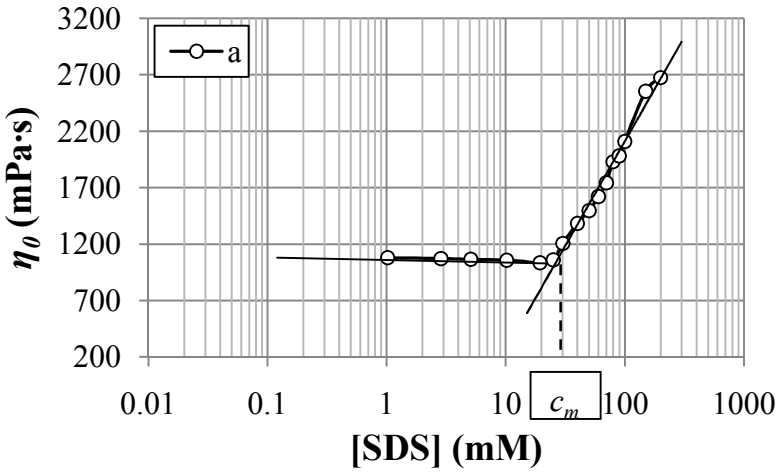

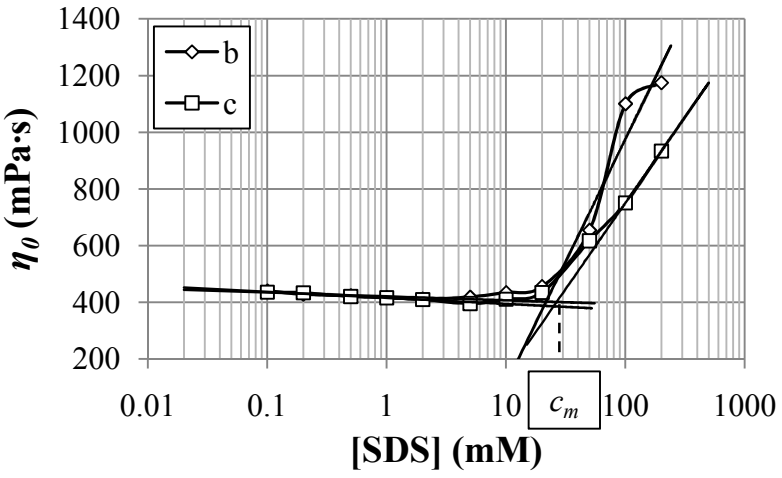

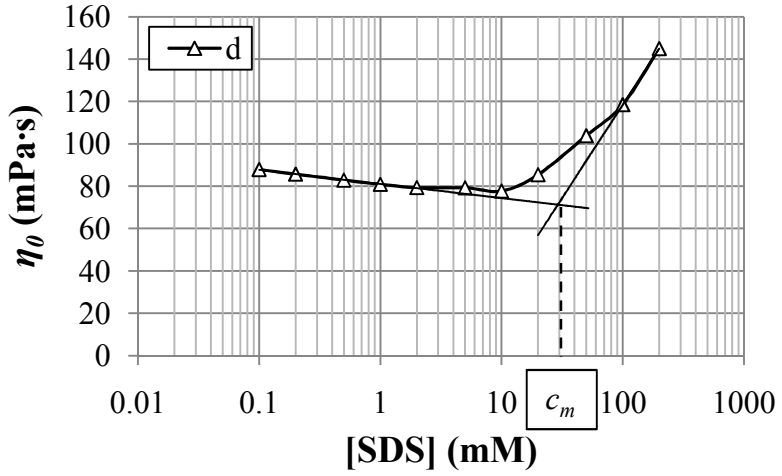

Figure 7 Zero-shear viscosity (η_0) of (a) 15%(w/v) PVP1300, (b) 10%(w/v) PVP1300, (c) 10%(w/v) PVP360, and (d) 30%(w/v) PVP55 solutions containing various SDS molar concentrations. The minimum effective surfactant concentration (c_m) for each polymer molecular grade and concentration is indicated.

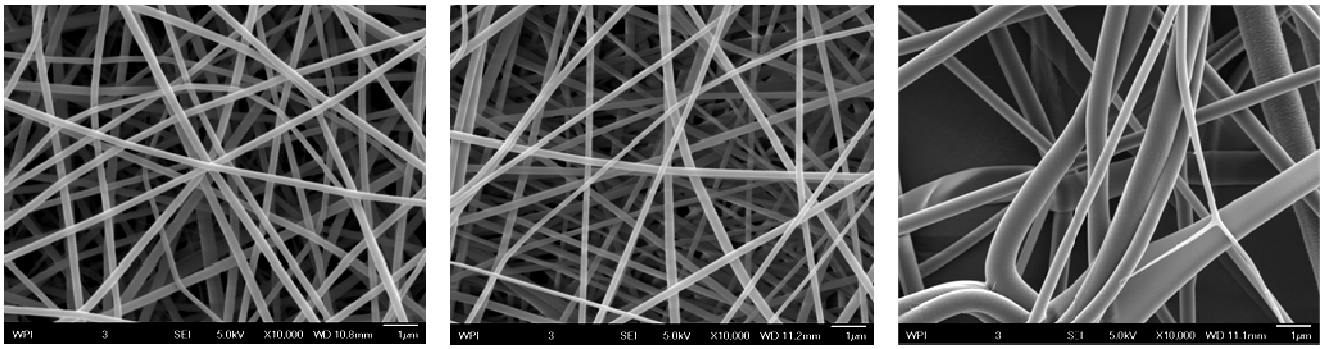

a-1 a-2 a-3

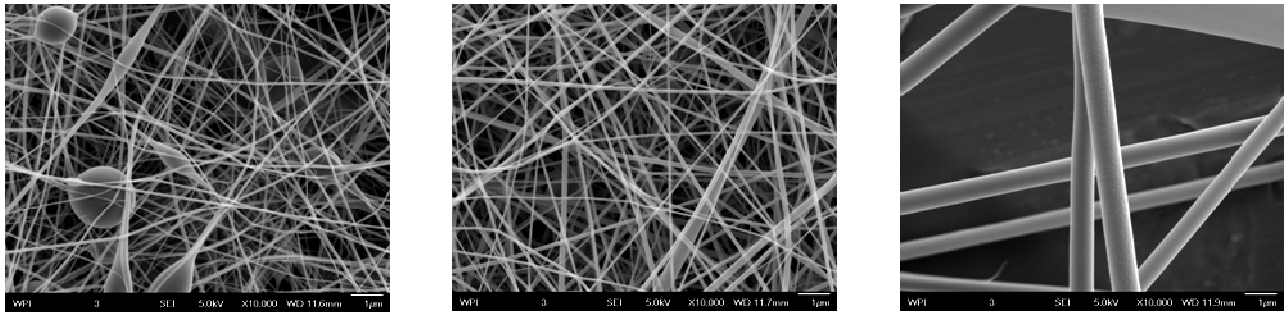

b-1 b-2 b-3

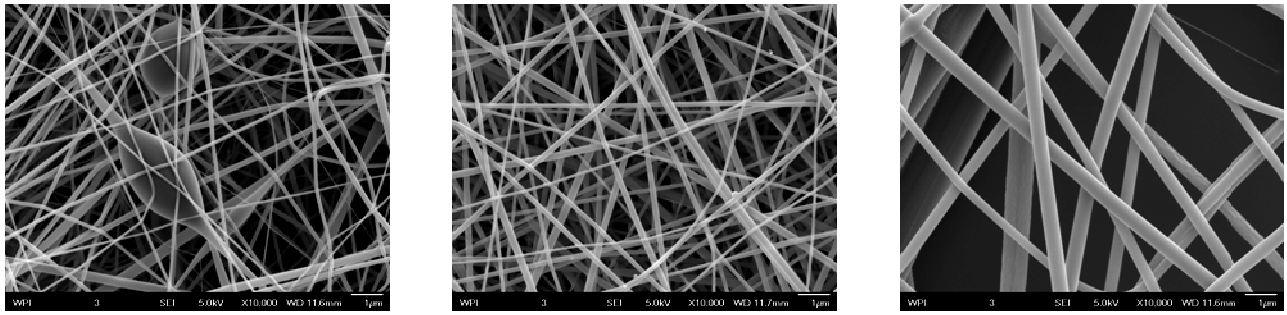

c-1 c-2 c-3

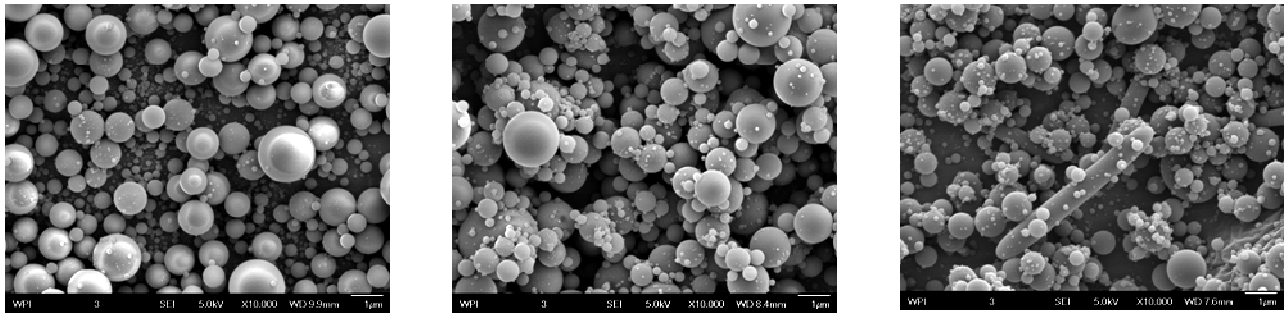

d-1 d-2 d-3

Figure 8 SEM micrographs of the electrospun structures from the precursors of (a)15%(w/v) PVP1300, (b)10%(w/v) PVP1300, (c) 10%(w/v) PVP360 and (d) 30%(w/v) PVP55 with various molar concentrations of SDS (1) 5 mM, (2) 20 mM, and (3) 200 mM.

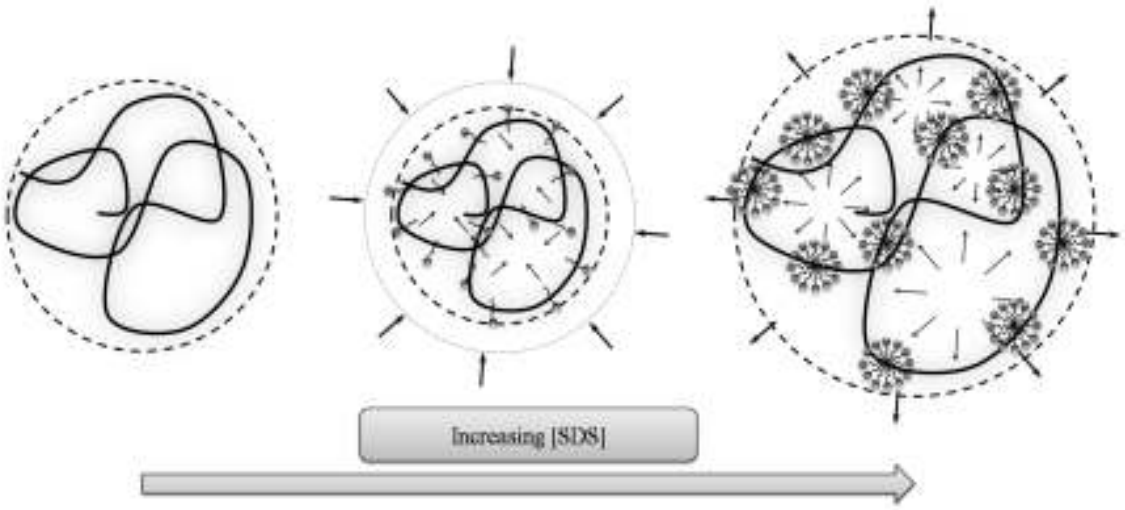

Figure 9 Schematic illustrations of the binding sequence between PVP and SDS in an aqueous solution at a constant polymer concentration constant and increasing SDS concentration. From the left, a regular polymer coil, the middle, the shrunk polymer coil due to the binding with surfactant anions, and the right, the expanded polymer coil due to the binding with the surfactant micelles.

CHAPTER 4 CONCLUSIONS

This thesis presents a series of papers that first show the successful development of a unique *in situ* forming hydrogel system. Several PEG diacrylate macromers were formulated with redox or photochemical initiators to provide hydrogels. Experimental results suggested hydrophobic modification is required to achieve low concentration aggregation and high polymerization efficiency. Photochemical polymerization is difficult to achieve in the absence of NVP as an accelerating co-monomer, particularly for macromers that lack hydrophobic modification. Swell data showed that when optimized to similarly high conversion, hydrogel network structure was most strongly influenced by macromer hydrophobicity and molecular weight.

Electrospinning technique was demonstrated as a versatile and efficient method to fabricate fibrous structures. Study of the fundamental parameter, polymer molecular weight distribution was exploited to establish the correlation between solution rheology and electrospun morphology. Using viscometry, the onset of entanglement concentrations with lower values were measured for the polydisperse polymer/solvent system. Intrinsic viscosity ($[\eta]$) was derived from viscometry results, which can be used to determine the effective molecular weight (M_E) controlling the solution viscosity. Results indicate that a higher moment of molecular weight (M_v) should be used to replace the weight average molecular weight in the historical rheological Mark-Houwink equation: $[\eta] = KM_w^a$. Fiber formation at low solution concentration was also observed during electrospinning. The results suggest that the presence of the high molecular weight fragments contribute to the early onset of fiber formation by enhancing the chain entanglements in the polydisperse polymer solutions.

Solution electrospinnability can also be improved by the addition of an anionic surfactant. The effects of molecular interactions between poly(vinylpyrrolidone) (PVP) and sodium dodecyl sulfate (SDS) on polymer coil dimension in their aqueous precursors and the electrospun morphology were investigated over a broad range of concentrations of the surfactant and as a function of three molecular weight grades of PVP. Viscometry was used to monitor the coil dimension. Results showed that SDS binds to the polymer chain and affects the PVP coil size through intramolecular interactions. Two stages of binding were observed and separated by a surfactant minimum effective concentration (c_m) regardless of the polymer molecular grades and concentration. At $c<c_m$, surfactant anions bind to the polymer molecule leading to the contraction of the polymer coil while at $c\geq c_m$, surfactant micelles bind to the polymer molecule resulting in the expansion of the coil. These solutions were electrospun and the morphologies were studied by scanning electron microscope (SEM). Pure PVP aqueous solutions deposited as beads or beaded fibrous structures and could be stabilized by the addition of surfactant. Experimental results demonstrated that in the moderately entangled solutions, above c_m, surfactant affected polymer solutions yielded fine uniform fibers. In the polymer solution with no entanglements, a decrease in uniformity was observed in the electrospun pattern with the addition of surfactant. This study demonstrated the versatility of electrospinning technique which, by including an additional component, enables the production of uniform fine fibrous structures at low polymer viscosity.